

The perfect lens & manipulating light on the nanoscale

John Pendry

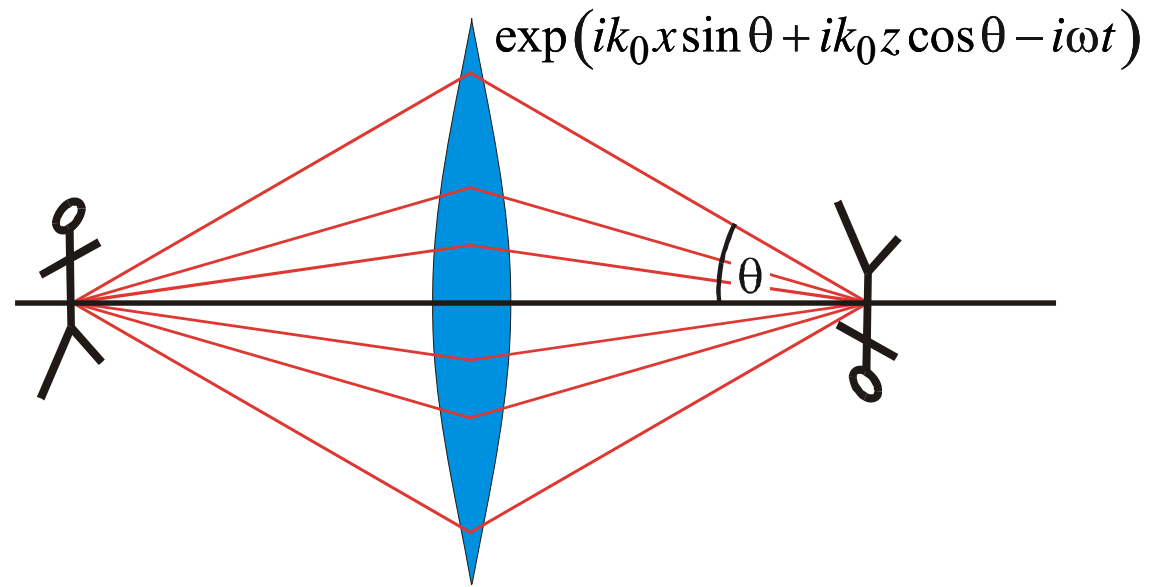
Imperial College London



Focussing light



Galileo by Leoni - 1624

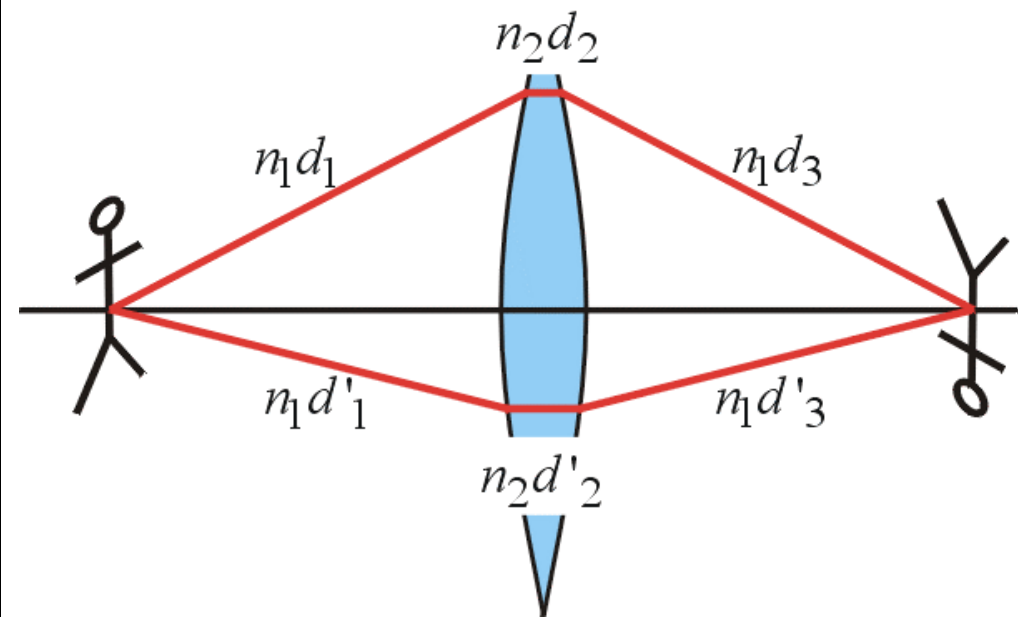


lens, *n.* *L. lens* lentil, from the similarity in form. A piece of glass with two curved surfaces

Fermat's Principle:



“Light takes the shortest optical path between two points”



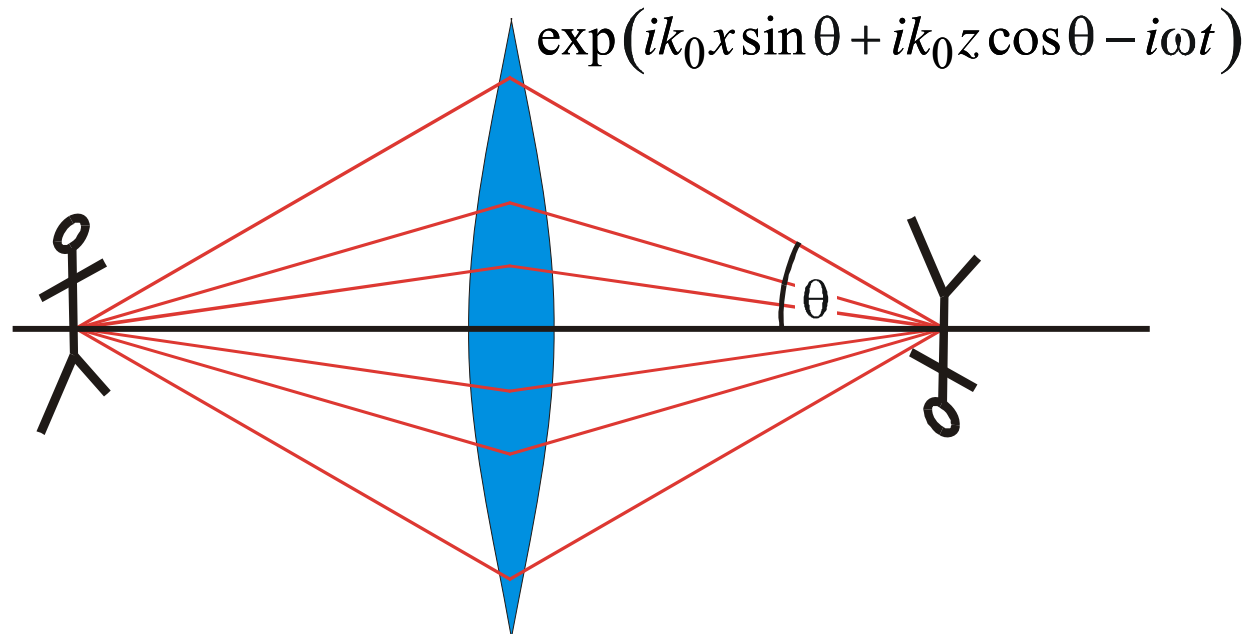
e.g. for a lens the shortest optical distance between object and image is:

$$n_1d_1 + n_2d_2 + n_1d_3 = n_1d'_1 + n_2d'_2 + n_1d'_3$$

both paths converge at the same point because both correspond to a minimum.

Focussing light: wavelength limits the resolution

Contributions of the far field to the image



..... are limited by the free space wavelength:

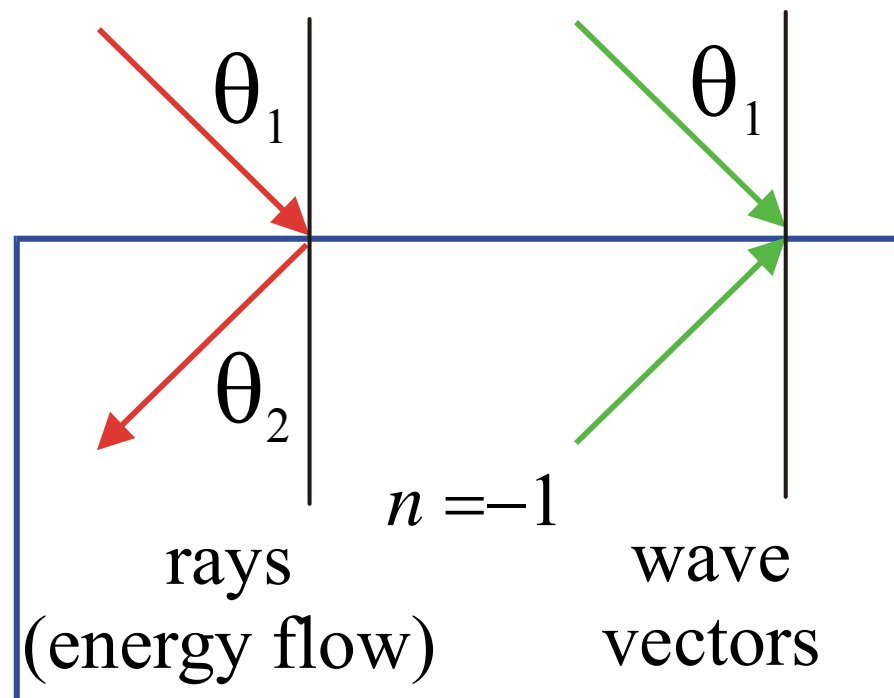
$\theta = 90^\circ$ gives maximum value of $k_x = k_0 = \omega/c_0 = 2\pi/\lambda_0$ – the shortest wavelength component of the 2D image. Hence resolution is no better than,

$$\Delta \approx \frac{2\pi}{k_0} = \frac{2\pi c}{\omega} = \lambda_0$$

Negative Refractive Index and Snell's Law

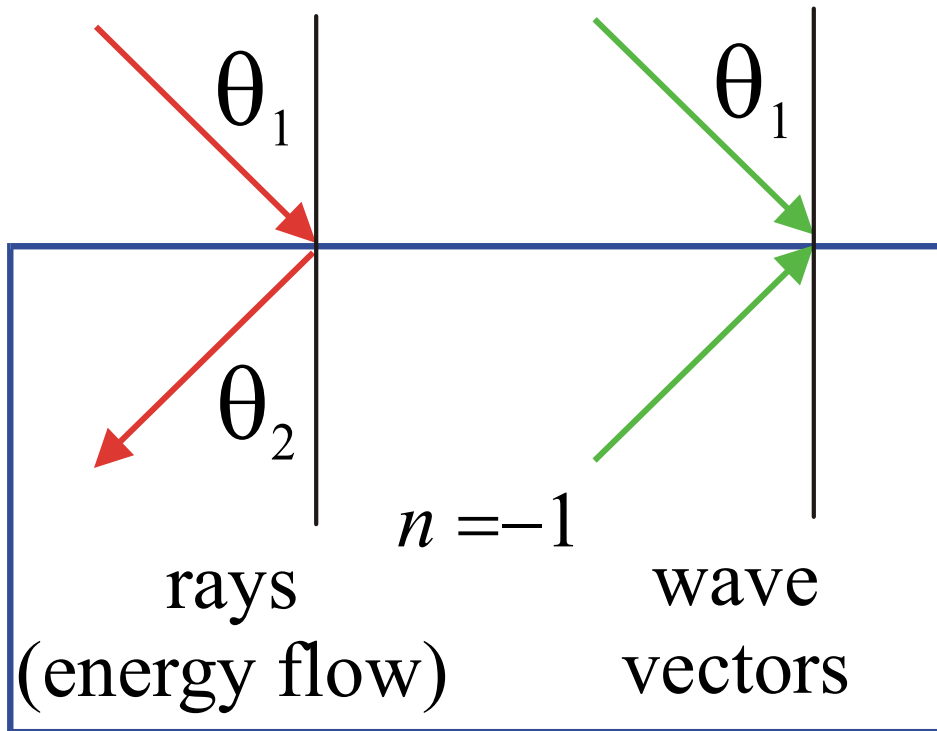
$$n = \frac{\sin(\theta_1)}{\sin(\theta_2)}$$

Hence in a negative refractive index material, *light makes a negative angle with the normal*. Note that the parallel component of wave vector is always preserved in transmission, but that energy flow is opposite to the wave vector.

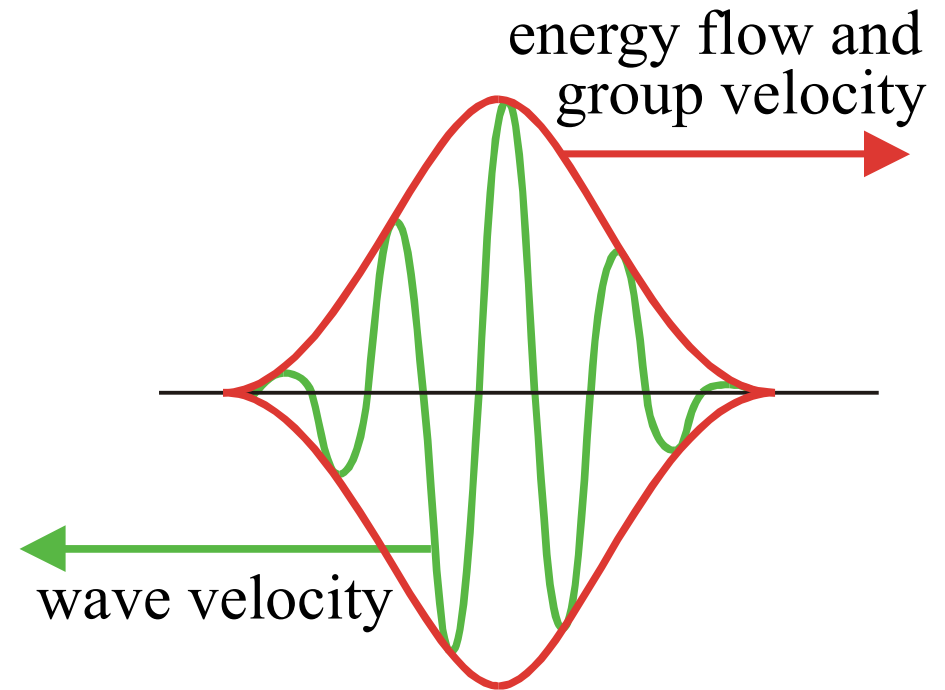


The consequences of negative refraction

1. negative group velocity

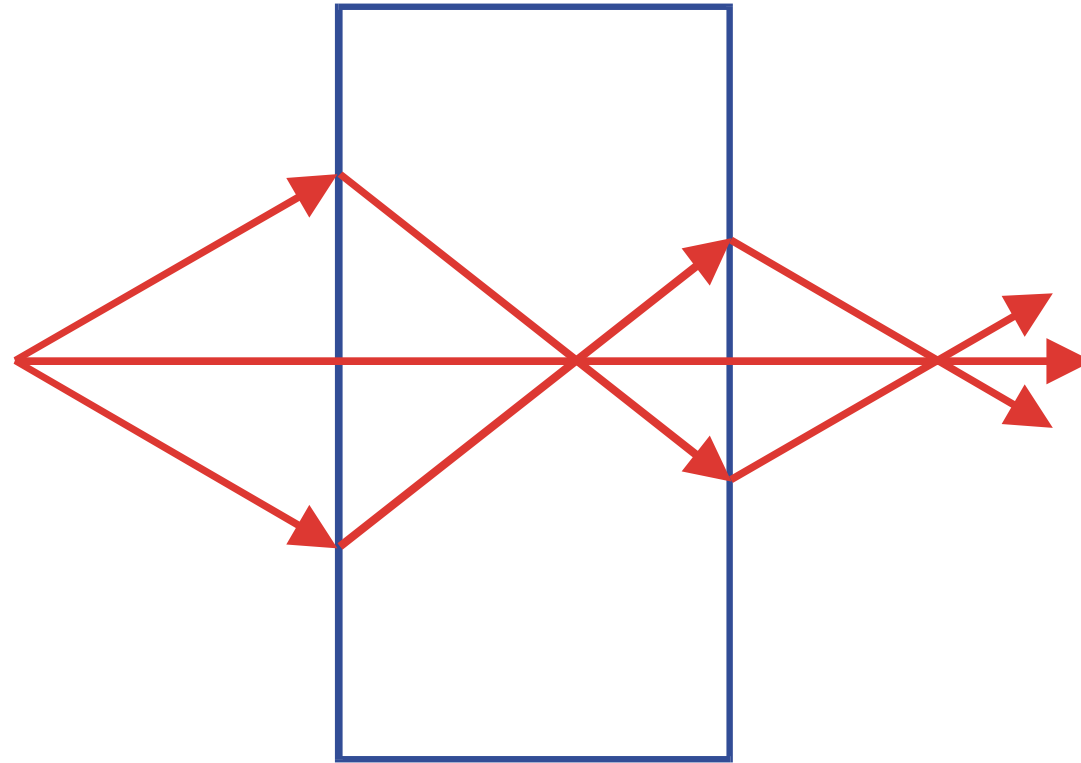


In a negative refractive index material, *light makes a negative angle with the normal*. Note that the parallel component of wave vector is always preserved in transmission, but that energy flow is opposite to the wave vector.



Materials with negative refraction are sometimes called *left handed materials* because the Poynting vector has the opposite sign to the wave vector.

Negative Refractive Index and Focussing



A negative refractive index medium bends light to a negative angle relative to the surface normal. Light formerly diverging from a point source is set in reverse and converges back to a point. Released from the medium the light reaches a focus for a second time.

Recipe for Negative Refractive Index

James Clark Maxwell showed that light is an electromagnetic wave and its refraction is determined by both:

the electrical permittivity, ϵ ,
and the magnetic permeability, μ .

The wave vector, k , is related to the frequency by the refractive index,

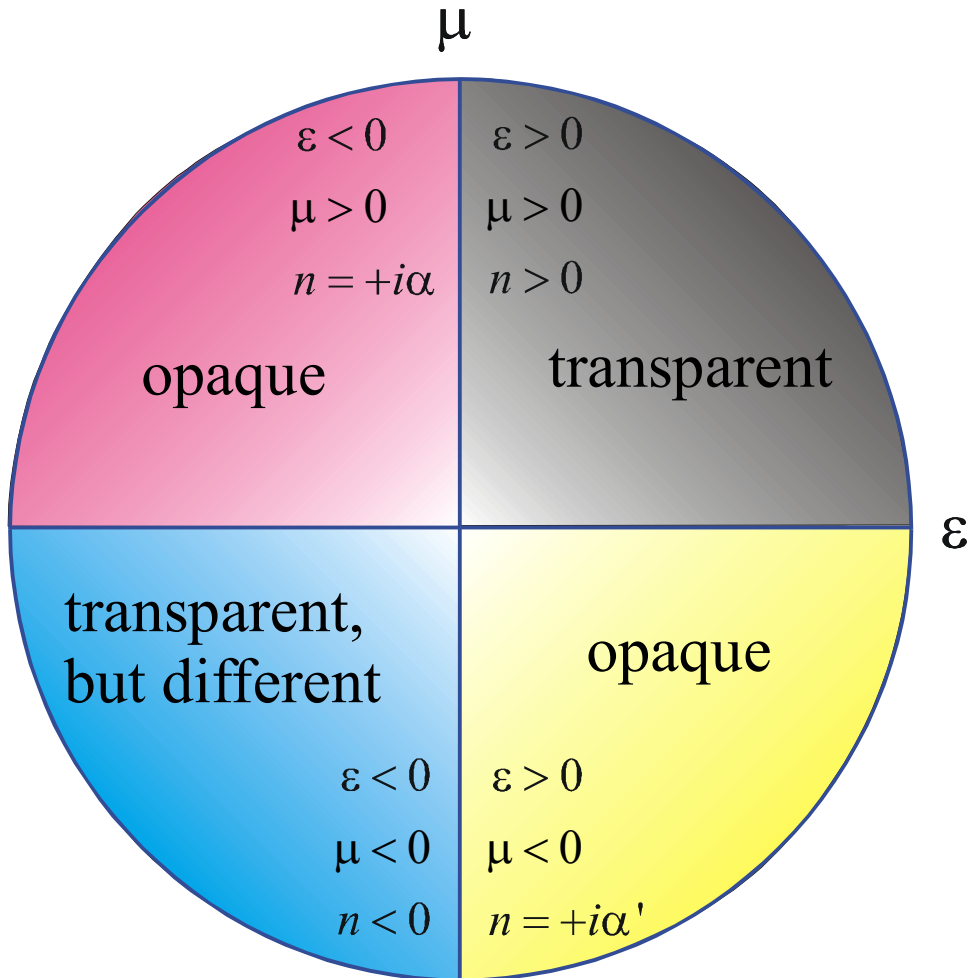
$$k = \sqrt{\epsilon\mu}\omega c_0^{-1} = n\omega c_0^{-1}$$

Normally n , ϵ , and μ are positive numbers.

In 1968 *Victor Veselago* showed that if ϵ and μ are negative, we are forced by Maxwell's equations to choose a negative square root for the refractive index,

$$n = -\sqrt{\epsilon\mu}, \quad \epsilon < 0, \quad \mu < 0$$

Negative Refraction - $n < 0$



where,

$$k = \omega/c \times \sqrt{\varepsilon\mu} = \omega/c \times n$$

Either $\varepsilon < 0$, or $\mu < 0$, ensures that k is imaginary, and the material opaque.

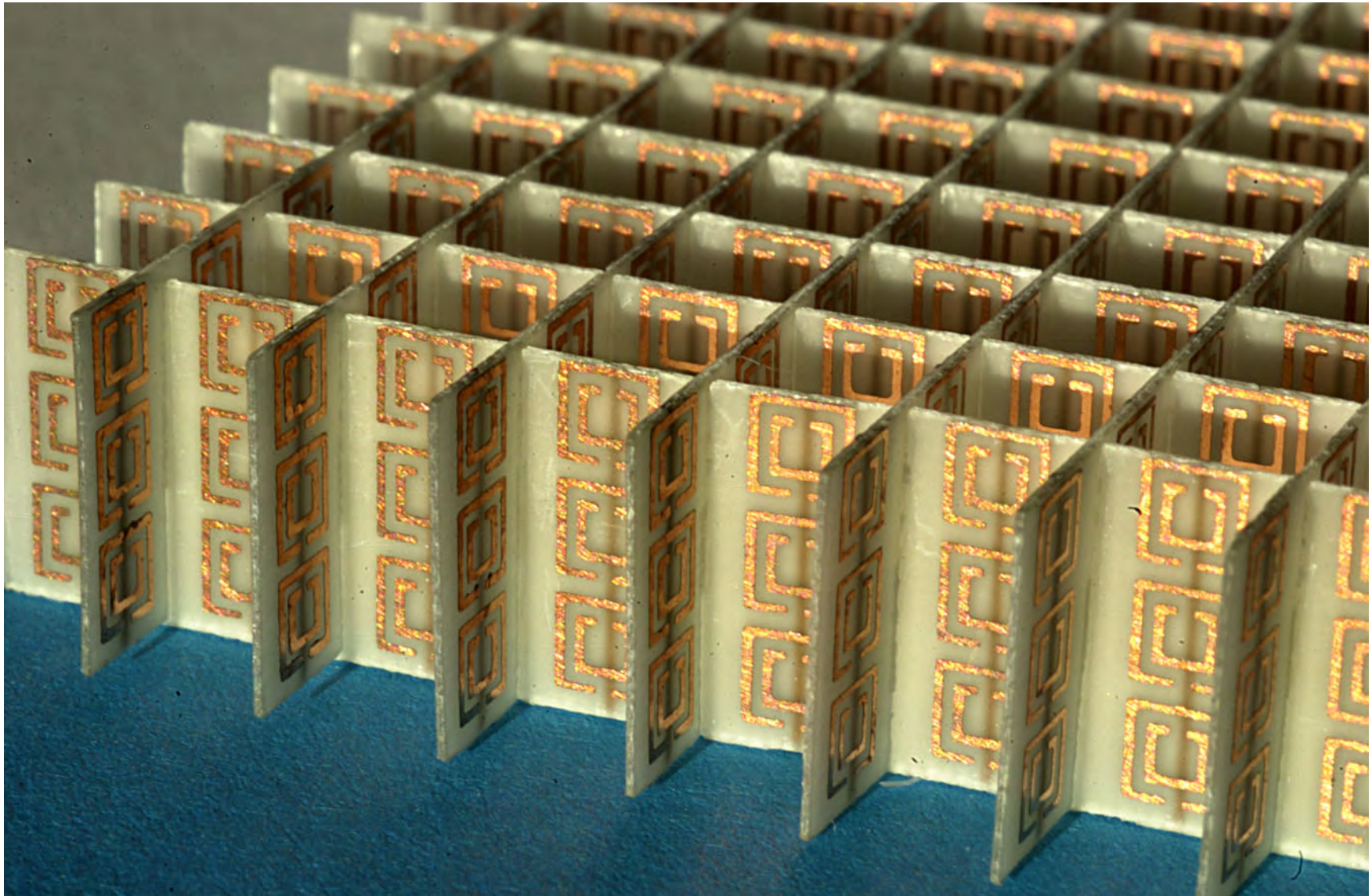
If $\varepsilon < 0$ and $\mu < 0$, then k is real, but we are forced to choose the *negative* square root to be consistent with Maxwell's equations.

$\varepsilon < 0, \mu < 0$ means that n is negative

The *wave vector* defines how light propagates:

$$E = E_0 \exp(ikz - i\omega t)$$

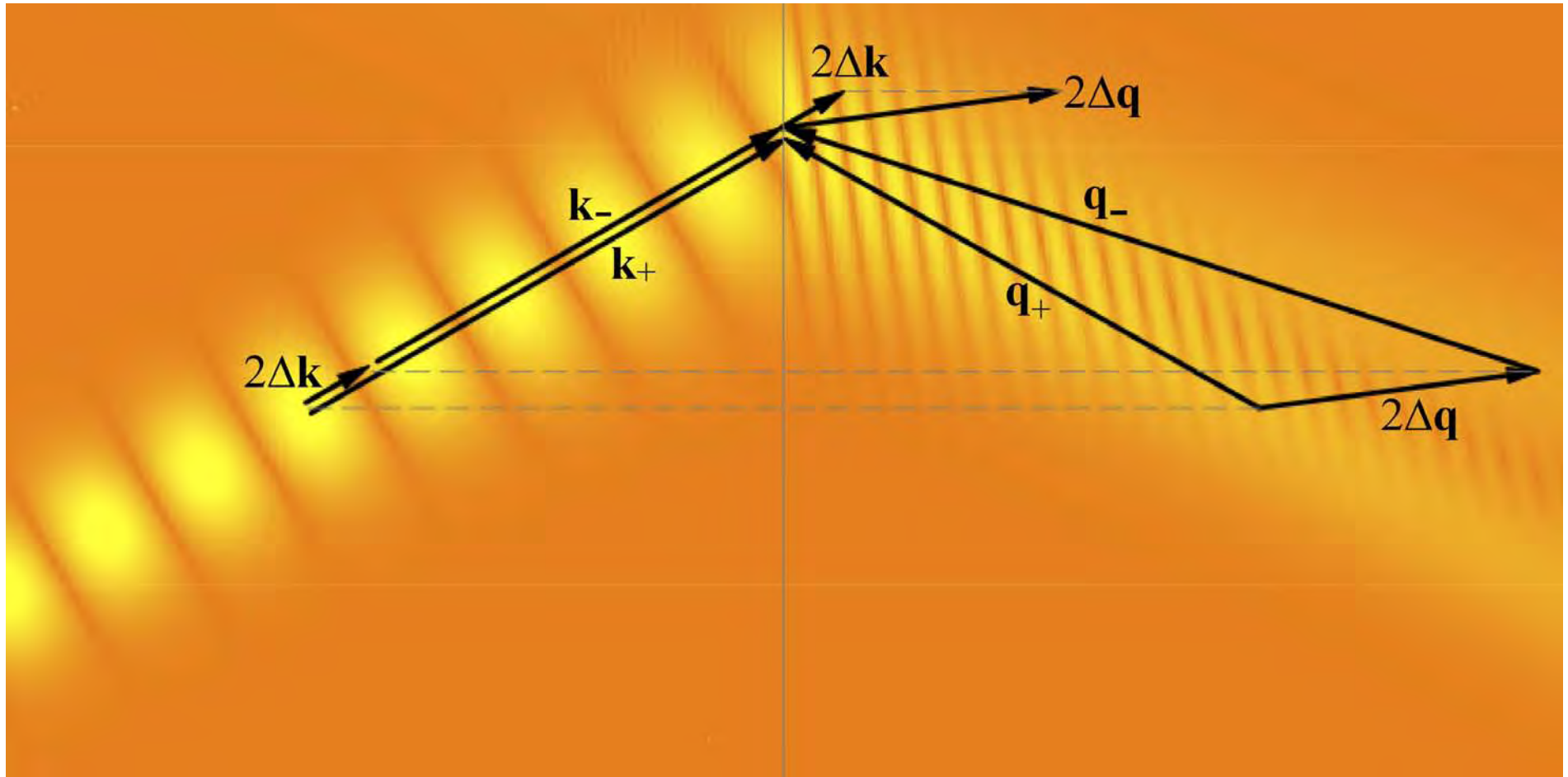
Negative refraction: $\epsilon < 0, \mu < 0$



Structure made at UCSD by David Smith

Refraction of a Gaussian beam into a negative index medium.

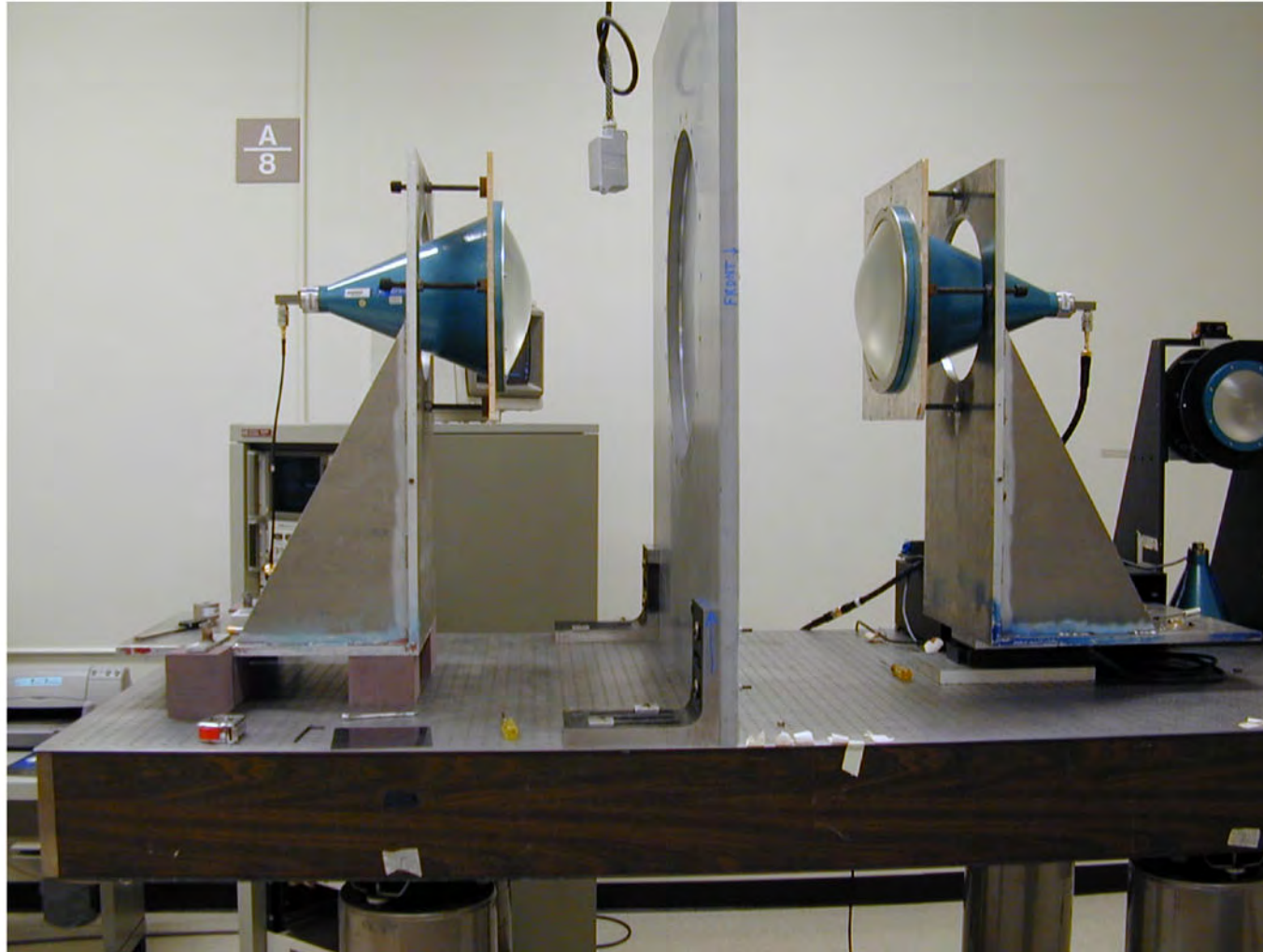
The angle of incidence is 30° (computer simulation by David Smith UCSD)



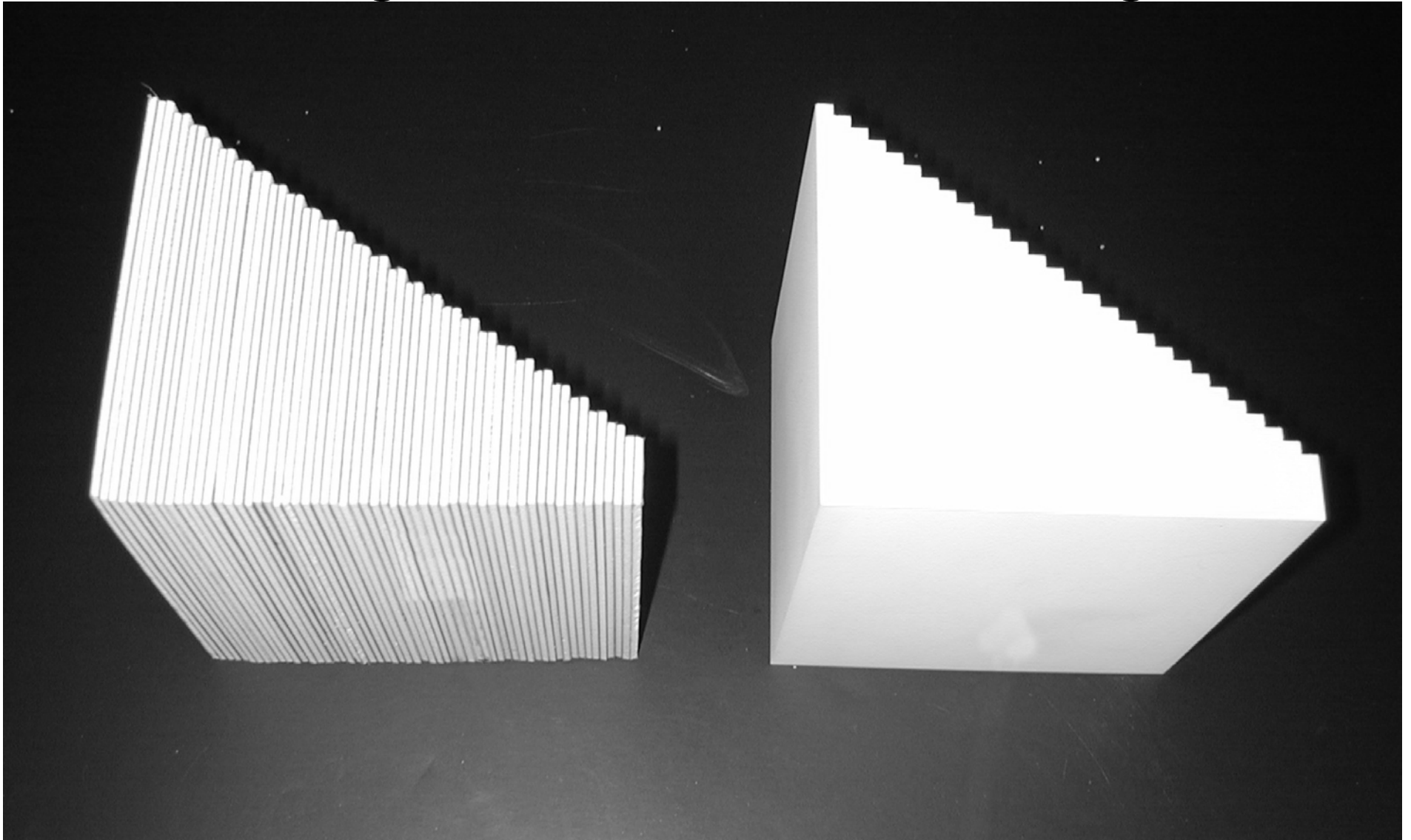
$$n(\omega_-) = -1.66 + 0.003i, \quad n(\omega_+) = -1.00 + 0.002i, \quad \Delta\omega/\omega = 0.07$$

Negative Refraction at the Phantom Works

Free-Space Experimental Set-up



Boeing Phantom Works 32° wedges



Left: negatively refracting sample

Right: teflon

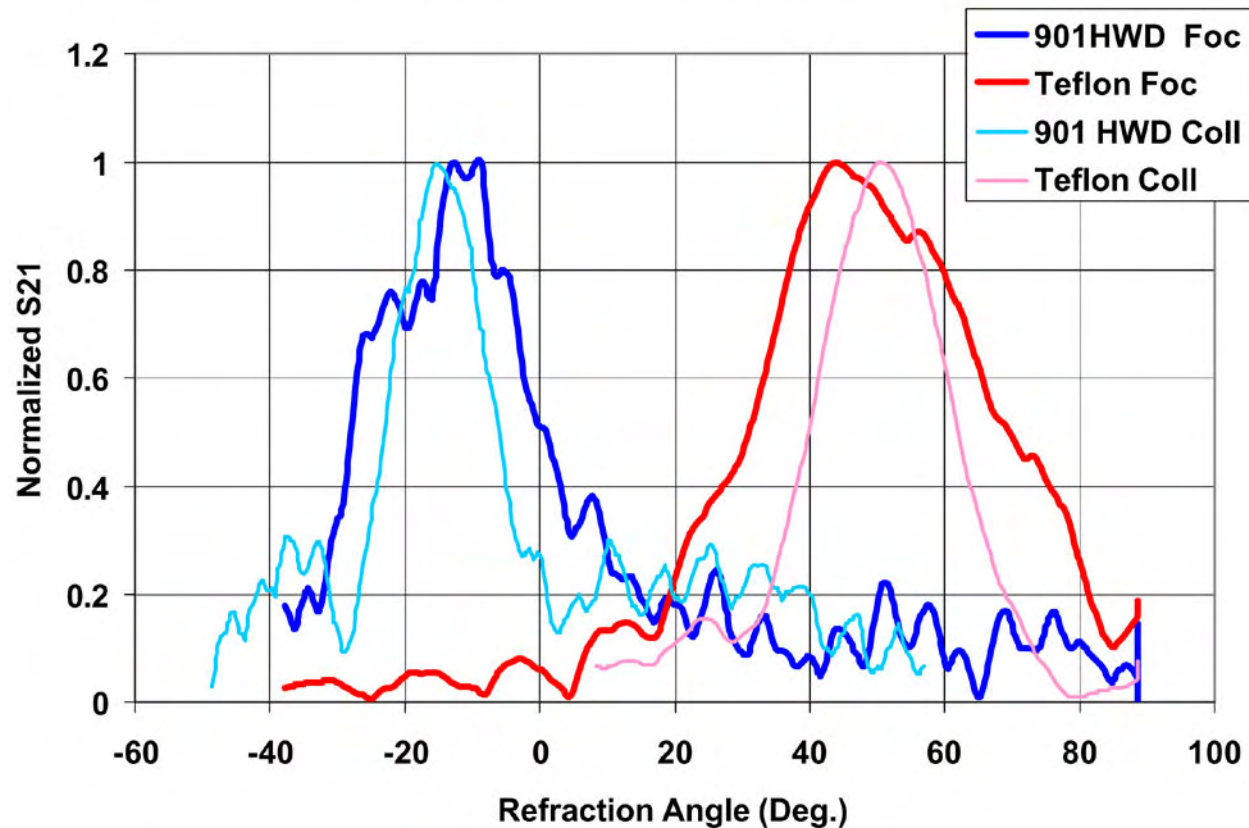


Snell's Law Verification for $n < 0$ in Free Space (2)

(Line plots, $f=13$ GHz, detector at 13", Boeing 2002)

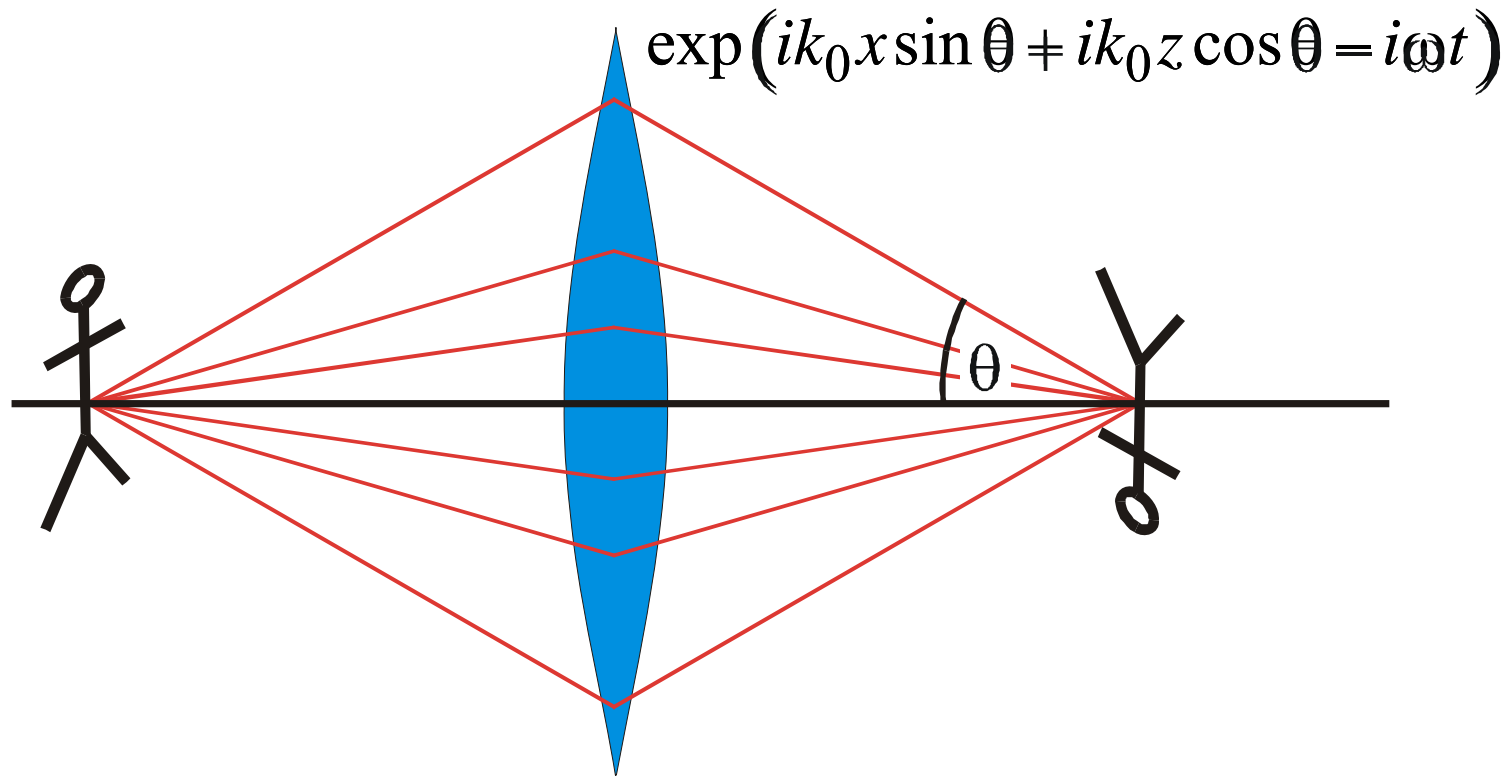


Snell's Law Focused & Collimated Data (13", 13GHz, 901HWD on Rogers)



Limitations to the Performance of a Lens

Contributions of the far field to the image



..... are limited by the free space wavelength: $\theta = 90^\circ$ gives maximum value of $k_x = k_0 = \omega/c_0 = 2\pi/\lambda_0$ – the shortest wavelength component of the 2D image. Hence resolution is no better than,

$$\Delta \approx \frac{2\pi}{k_0} = \frac{2\pi c}{\omega} = \lambda_0$$

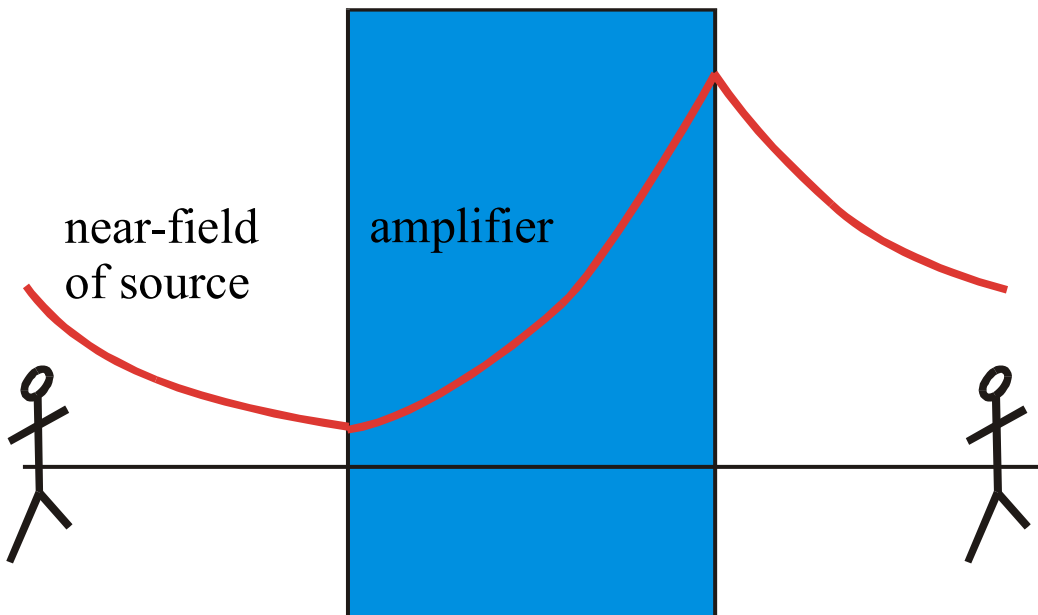
Limitations to a Conventional Lens (2)

Contributions of the near field to the image

come from large values of k_x responsible for the finest details in the source. Forget about ray diagrams because,

$$k_z = +i\sqrt{k_x^2 - \omega^2 c_0^{-2}}, \quad \omega^2 c_0^{-2} < k_x^2$$

and 'near field' light decays exponentially with distance from the source. i.e. the near field is confined to the immediate vicinity of the source. Unless we can make an *amplifier* it is inevitable that the finest detail is lost from the image.



Attempting the impossible:
a lens for the near field,
a negative story

The consequences of negative refraction

3. *Perfect* Focussing

A conventional lens has resolution limited by the wavelength. The missing information resides in the near fields which are strongly localised near the object and cannot be focussed in the normal way.

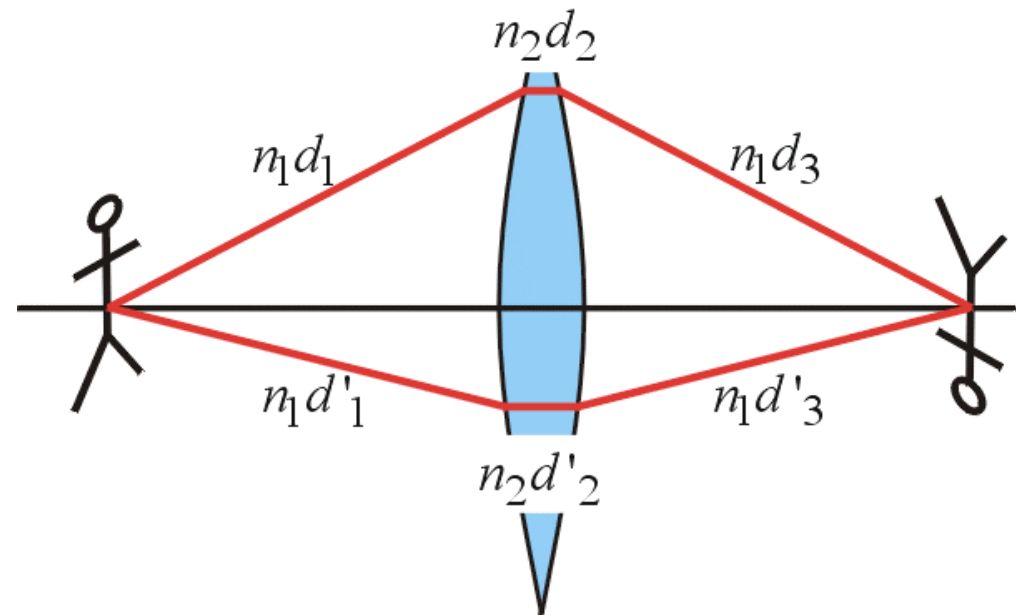
The new lens based on negative refraction has *unlimited resolution* provided that the condition $n = -1$ is met exactly. This can happen only at one frequency. (Pendry 2000).

The secret of the new lens is that it can focus the near field and to do this it must *amplify* the highly localised near field to reproduce the correct amplitude at the image.

Fermat's Principle:



“Light takes the shortest optical path between two points”



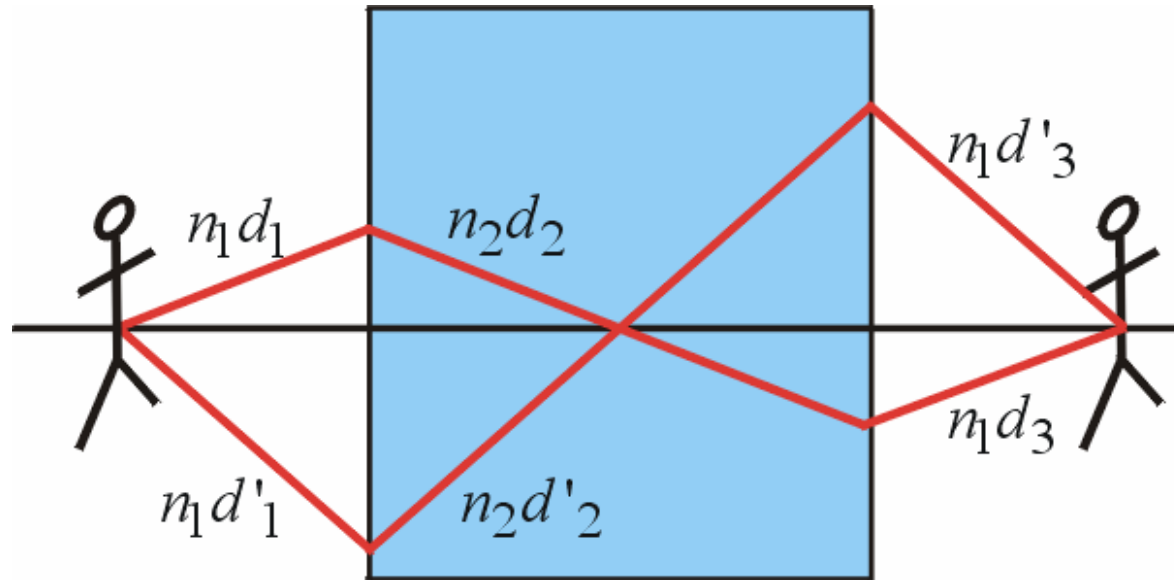
e.g. for a lens the shortest optical distance between object and image is:

$$n_1d_1 + n_2d_2 + n_1d_3 = n_1d'_1 + n_2d'_2 + n_1d'_3$$

both paths converge at the same point because both correspond to a minimum.

Fermat's Principle for Negative Refraction

If n_2 is negative the ray traverses **negative optical space**.



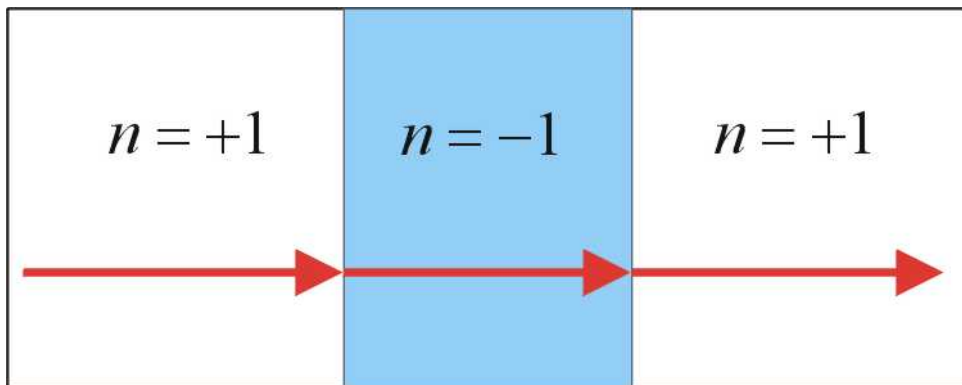
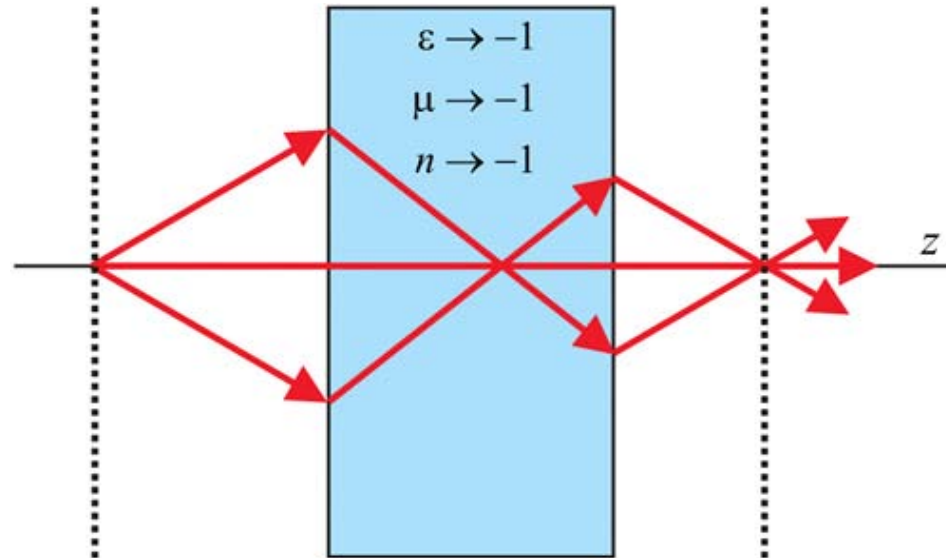
for a *perfect* lens ($n_2 = -n_1$) the shortest optical distance between object and image is **zero**:

$$\begin{aligned} 0 &= n_1 d_1 + n_2 d_2 + n_1 d_3 \\ &= n_1 d'_1 + n_2 d'_2 + n_1 d'_3 \end{aligned}$$

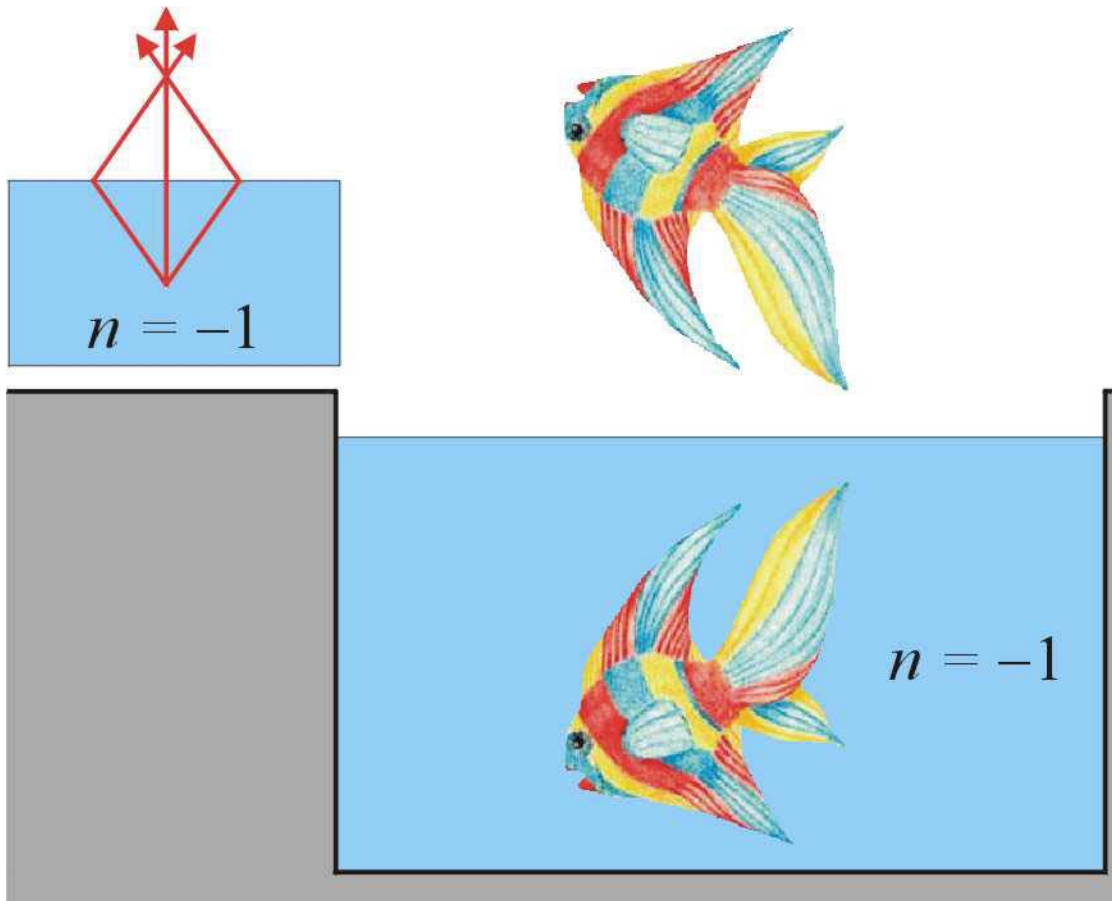
For a perfect lens the image *is* the object

Transformation optics & negative refraction

The Veselago lens can be understood in terms of transformation optics if we allow 'space' to take on a negative quality i.e. space can double back on itself so that a given event exists on several manifolds:



Bending light the wrong way

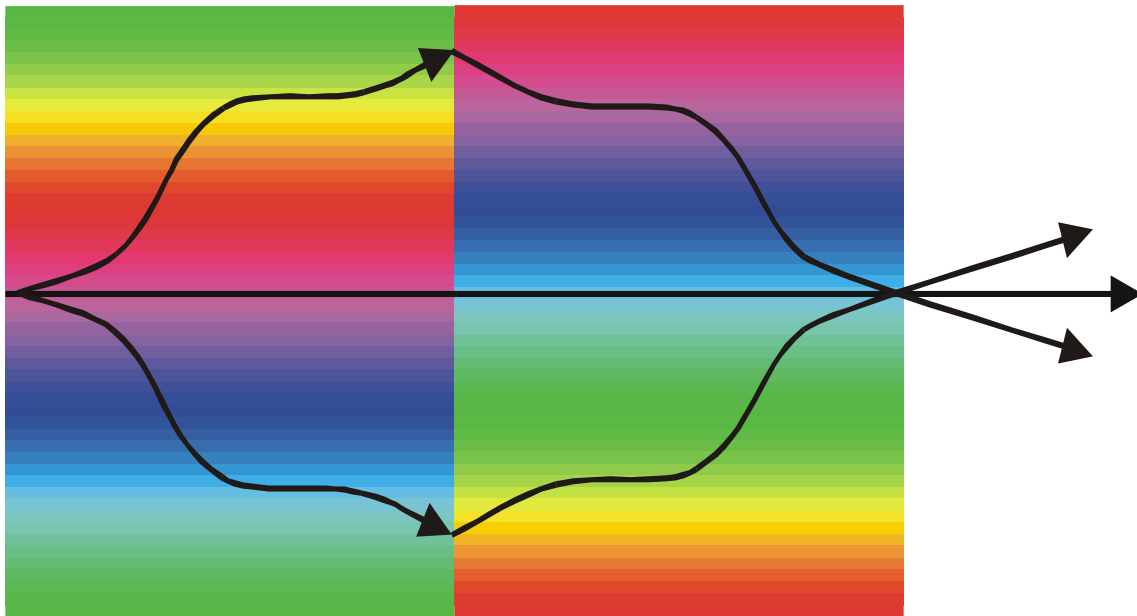


Negative refraction bends light ‘the wrong way’ at an interface (see inset top left) and as a result can refocus light as it emerges from a negatively refracting medium into air.

This implies that objects such as fish swimming in a negatively refracting fluid appear to an external observer to be floating in the air above

Negative Space

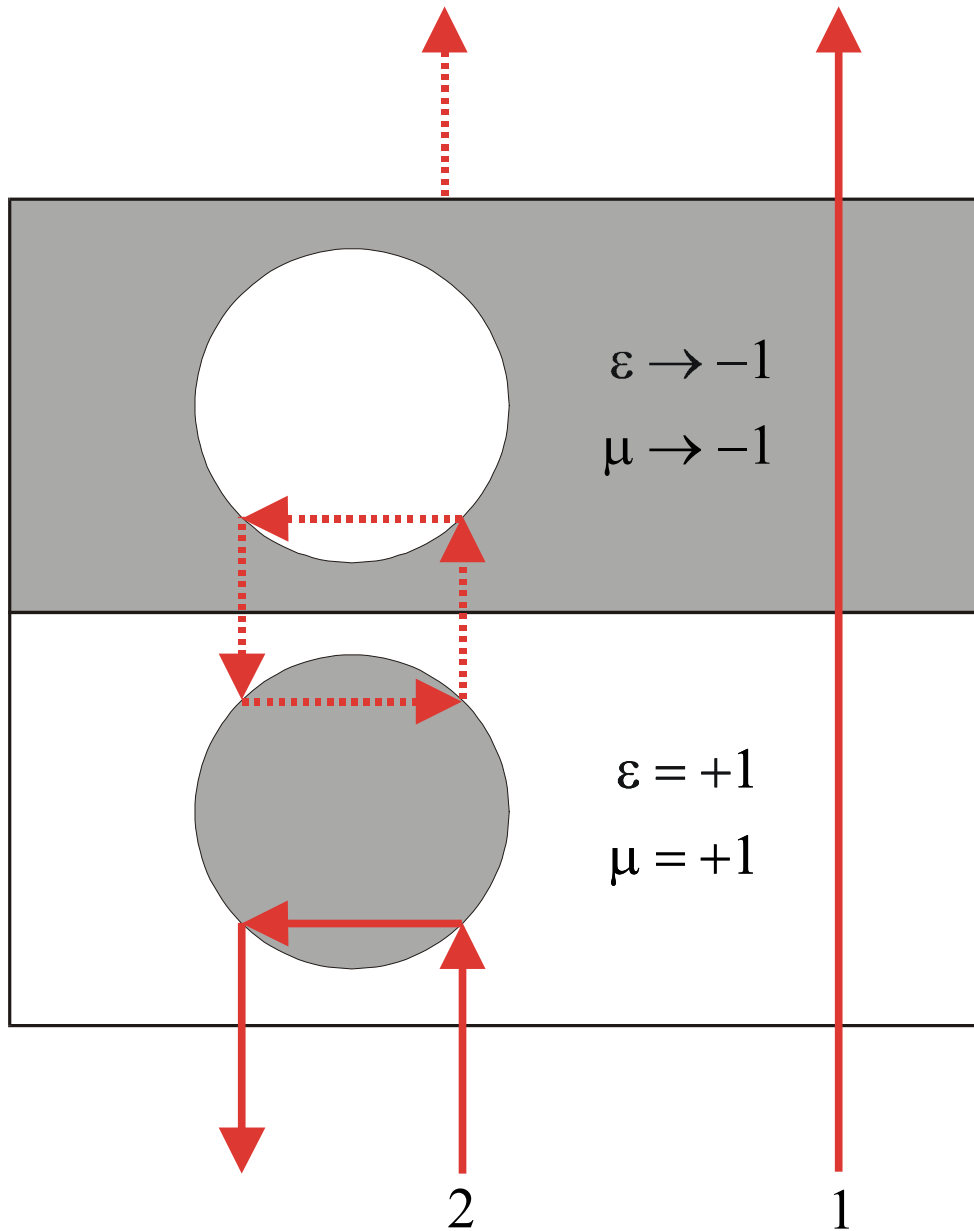
A slab of $n = -1$ material thickness d , cancels the effect of an equivalent thickness of free space. i.e. objects are focussed a distance $2d$ away. An alternative pair of complementary media, each cancelling the effect of the other. The light does not necessarily follow a straight line path in each medium:



General rule:
two regions of space
optically cancel if in each
region ϵ, μ are reversed
mirror images.

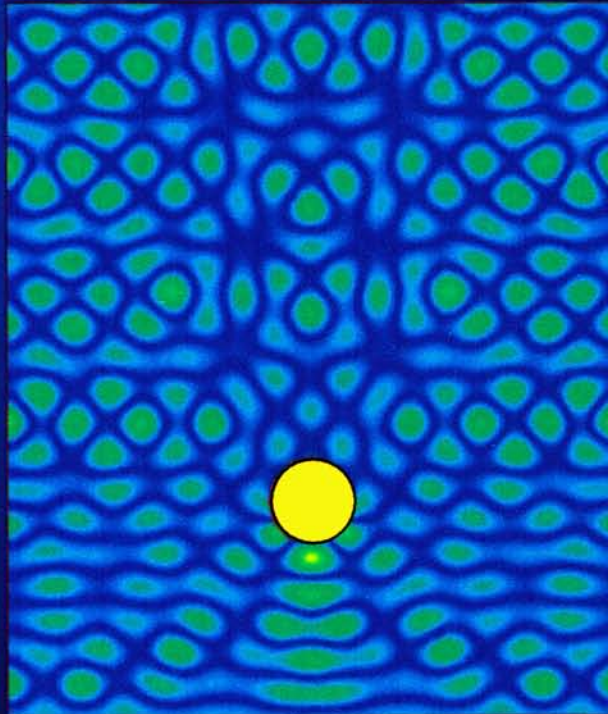
The overall effect is as if a section of space thickness $2d$ were removed from the experiment.

A Negative Paradox

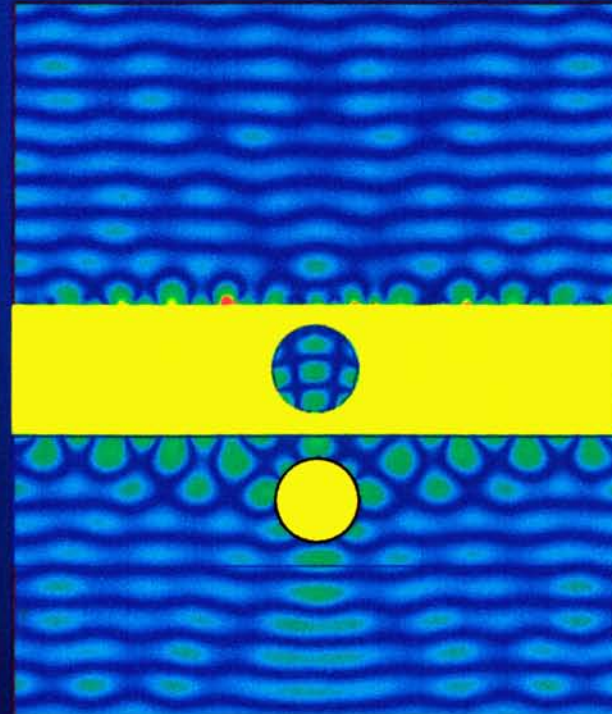


The left and right media in this 2D system are negative mirror images and therefore optically annihilate one another. However a ray construction appears to contradict this result. Nevertheless the theorem is correct and the ray construction erroneous. Note the closed loop of rays indicating the presence of resonances.

Compensation of inhomogeneous media



Scattering from a cylinder with $n=-1.4$



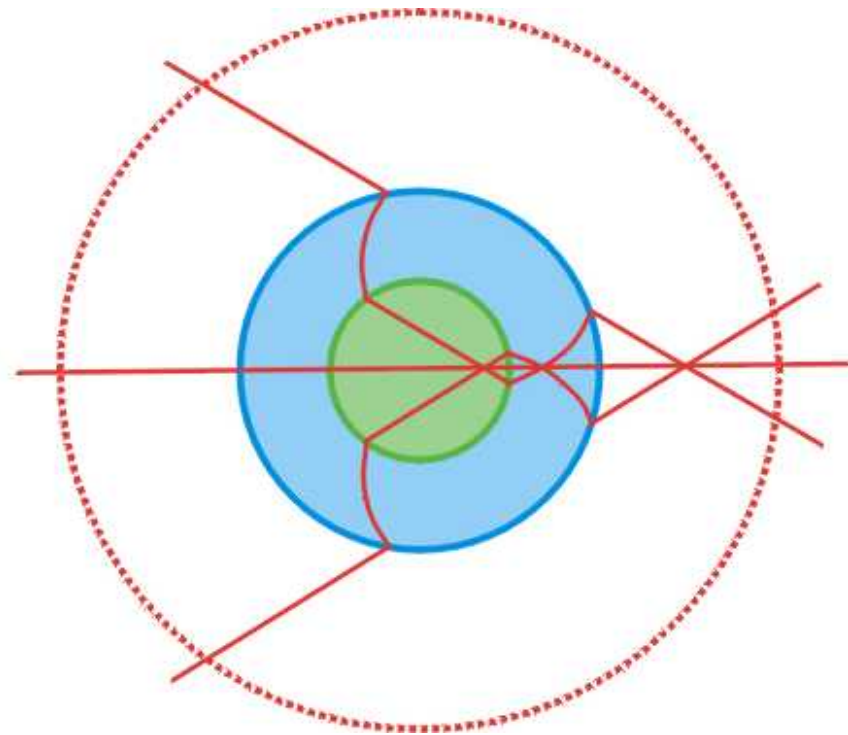
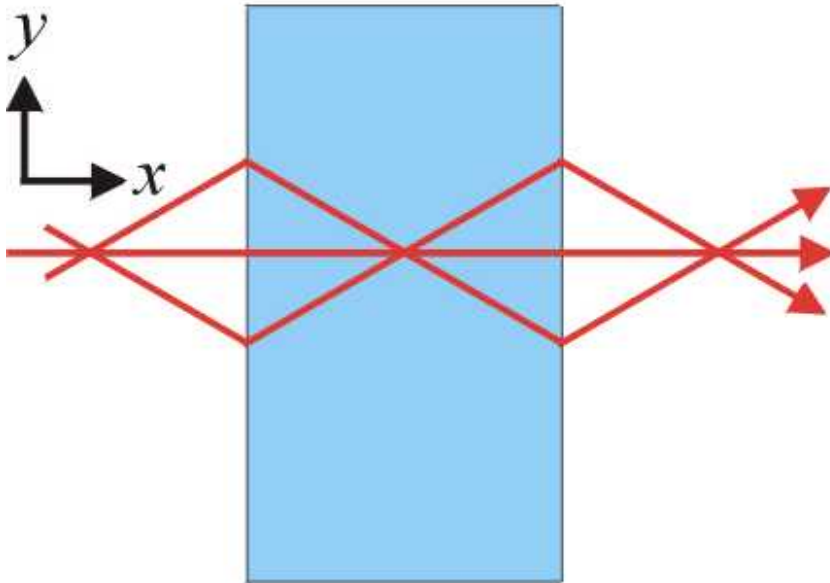
Compensation of the $n=-1.4$ cylinder

Cylindrical/Spherical lenses

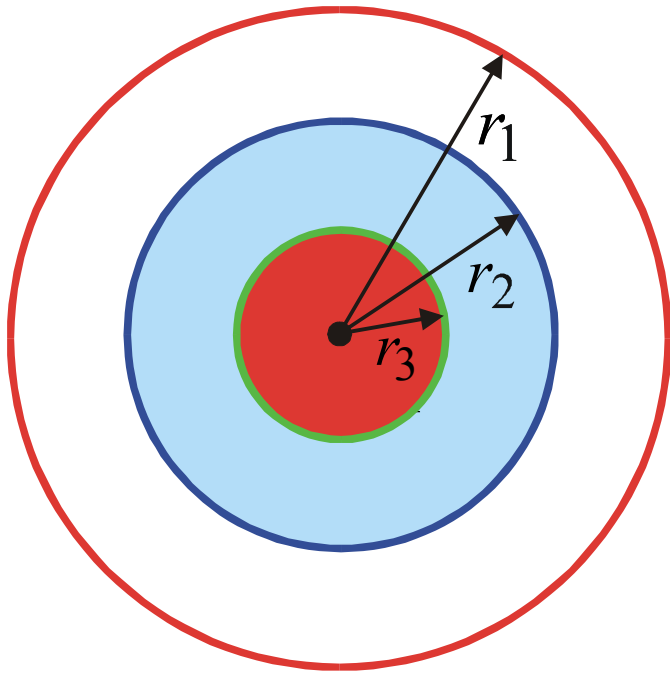
2003 Astron contract “Application of –ve materials to narrow beam antennae”
US Army funded – David Smith & John Pendry

Transformation optics was used to design the first spherical version of the Veselago lens i.e. ‘perfect’ magnification became possible using the transformation (cylindrical case),

$$r' = \frac{1}{2} \ln(x^2 + y^2), \quad \theta' = \arctan(y/x), \quad z' = z$$



A Perfect Magnifying Glass



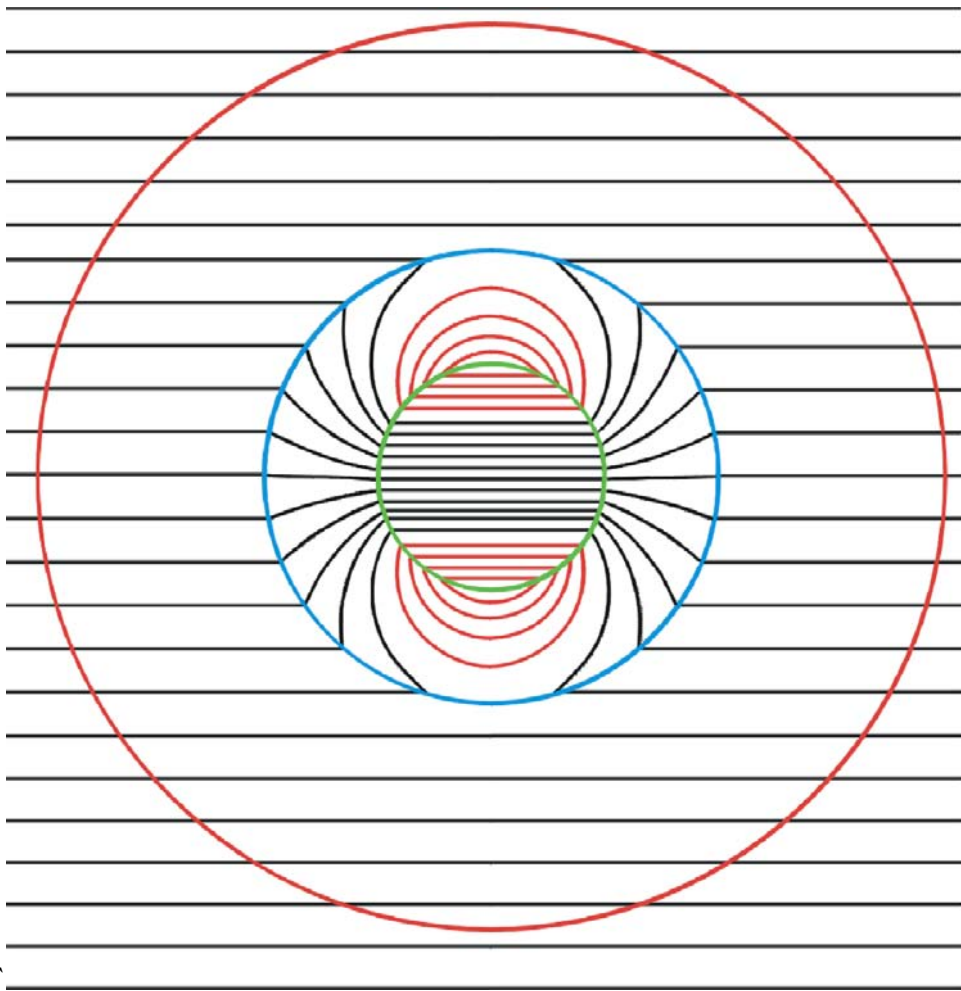
$$\epsilon_x = \epsilon_y = \epsilon_z = +\frac{r_2^2}{r_3^2}, \quad 0 < r < r_3$$

$$\epsilon_x = \epsilon_y = \epsilon_z \rightarrow -\frac{r_2^2}{r^2}, \quad r_3 < r < r_2$$

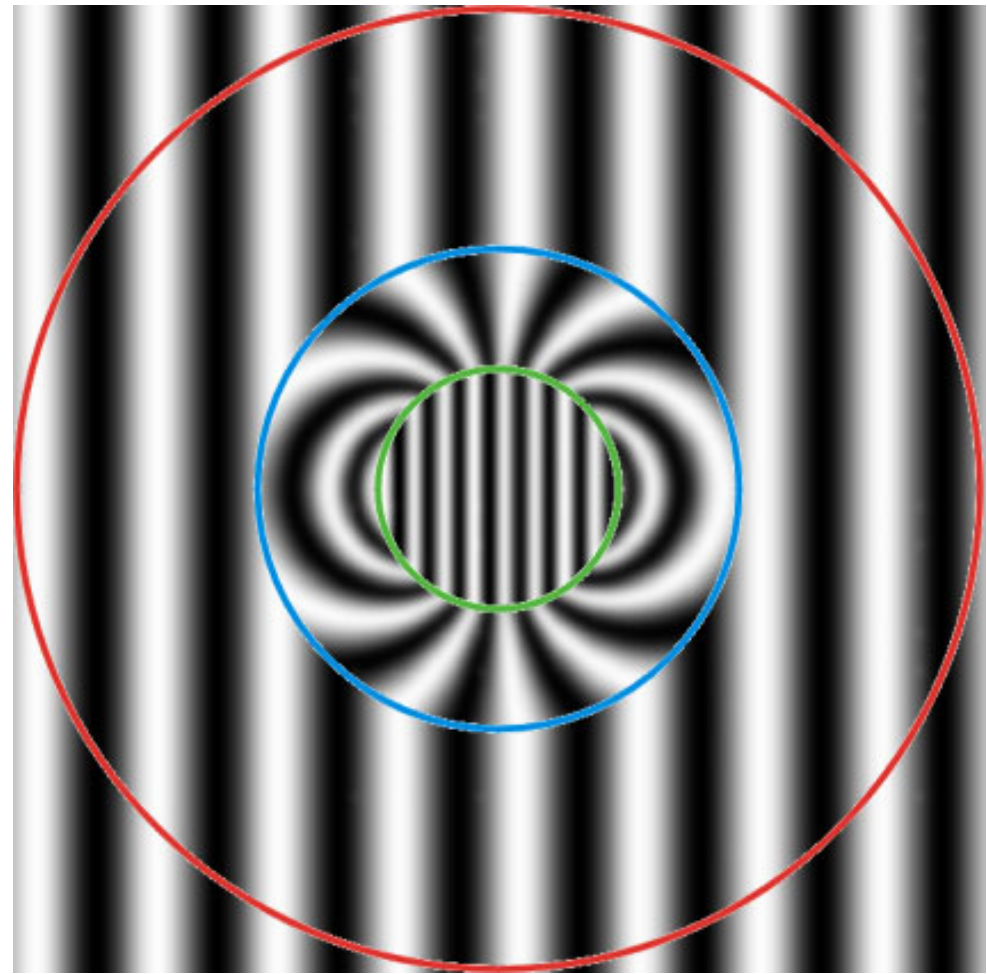
$$\epsilon_x = \epsilon_y = \epsilon_z = +1, \quad r_2 < r < \infty$$

$$\mu_x = \epsilon_x, \quad \mu_y = \epsilon_y, \quad \mu_z = \epsilon_z$$

It is possible to design a spherical annulus of negative material lying between r_2 and r_3 that acts like a magnifying glass. To the outside world the contents of the sphere radius r_3 appear to fill the larger sphere radius r_1 with proportionate magnification.



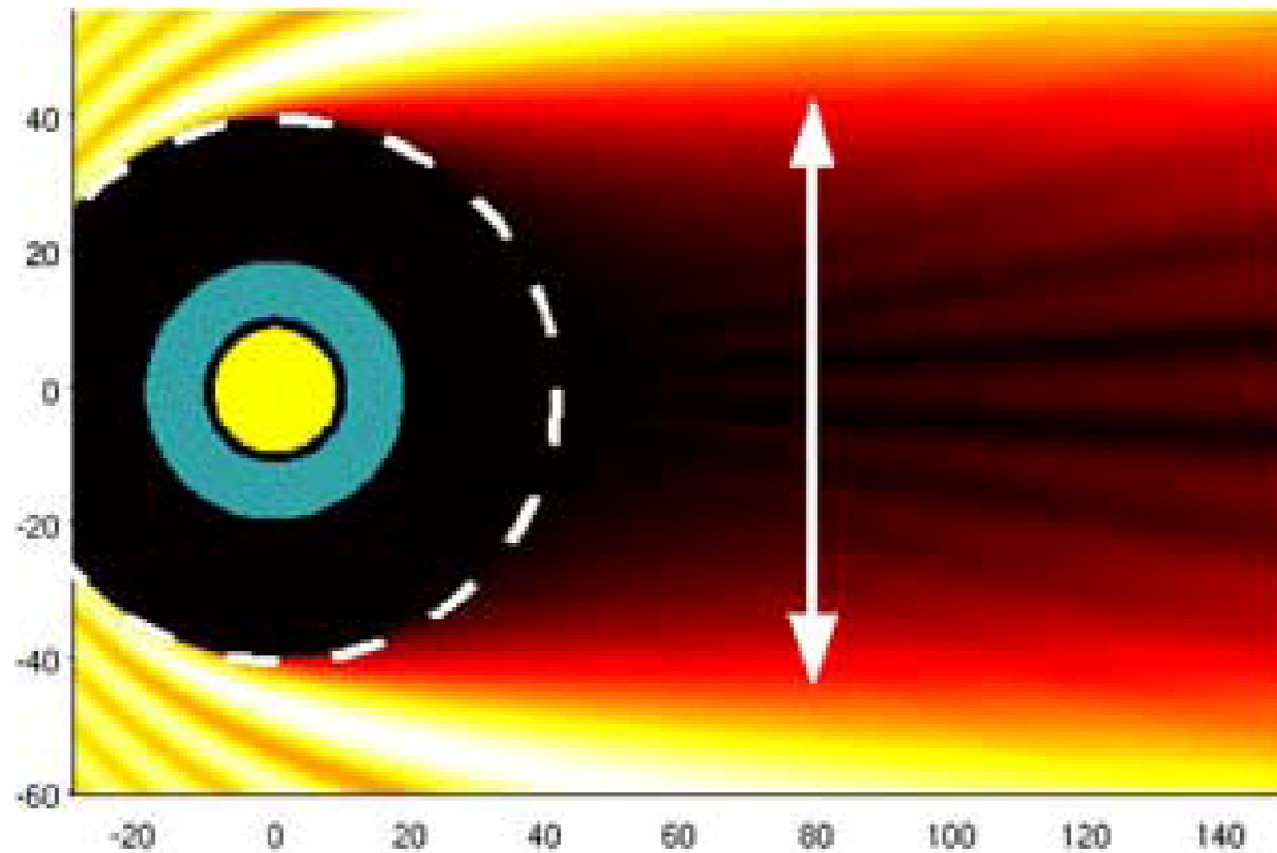
1a)



1b)

An optical turbine. A plane wave entering the red sphere from the left is captured and compressed inside the green sphere. **a)** A ray picture which shows only part of the rays being captured **b)** An exact solution of Maxwell's equations. The green sphere is filled with the compressed contents of the red sphere as predicted. The region outside the blue sphere is free space.

Transformation Optics Shrinks Optical Devices: a shadow created by a sub wavelength device



yellow inner cylinder: perfectly absorbing material

blue annulus: magnifying superlens – radius about one wavelength

The device creates a deep shadow in light incident from the left. **The shadow is far bigger than the physical device creating it. How can this happen?**

The 'Poor Man's Superlens'

The original prescription for a superlens: a slab of material with

$$\varepsilon = -1, \mu = -1$$

However if all relevant dimensions (the thickness of the lens, the size of the object etcetera) are much less than the wavelength of light, electric and magnetic fields are decoupled. An object that comprises a pure electric field can be imaged using a material with,

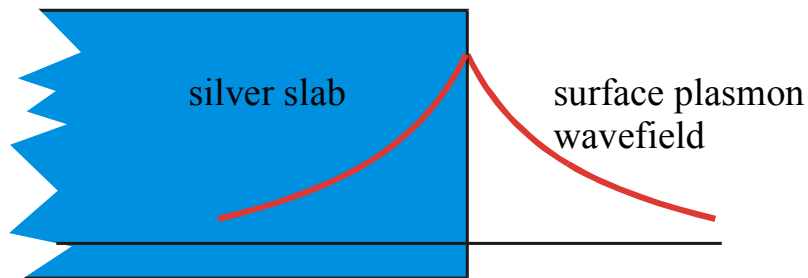
$$\varepsilon = -1, \mu = +1$$

because, in the absence of a magnetic field, μ is irrelevant.

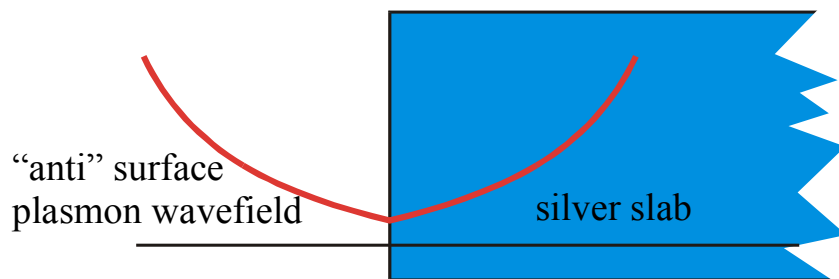
We can achieve this with a slab of silver which has $\varepsilon < 0$ at optical frequencies.

Anatomy of a Superlens

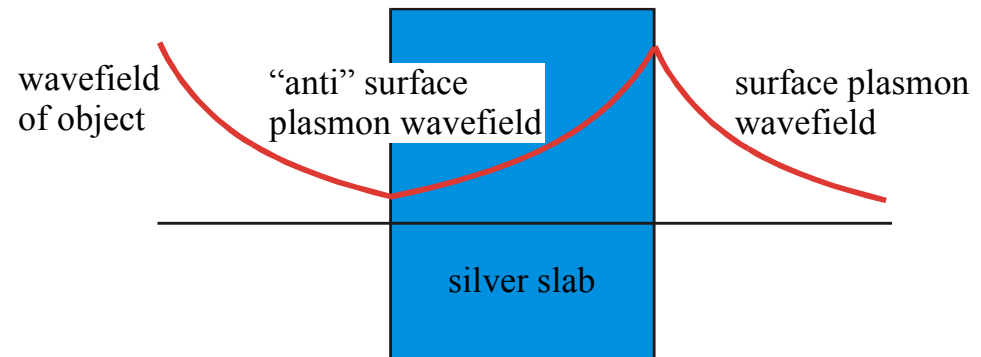
The superlens works by **resonant excitation of surface plasmons in the silver**,



At the same frequency as the surface plasmon there exists an unphysical "anti" surface plasmon - wrong boundary conditions at infinity,



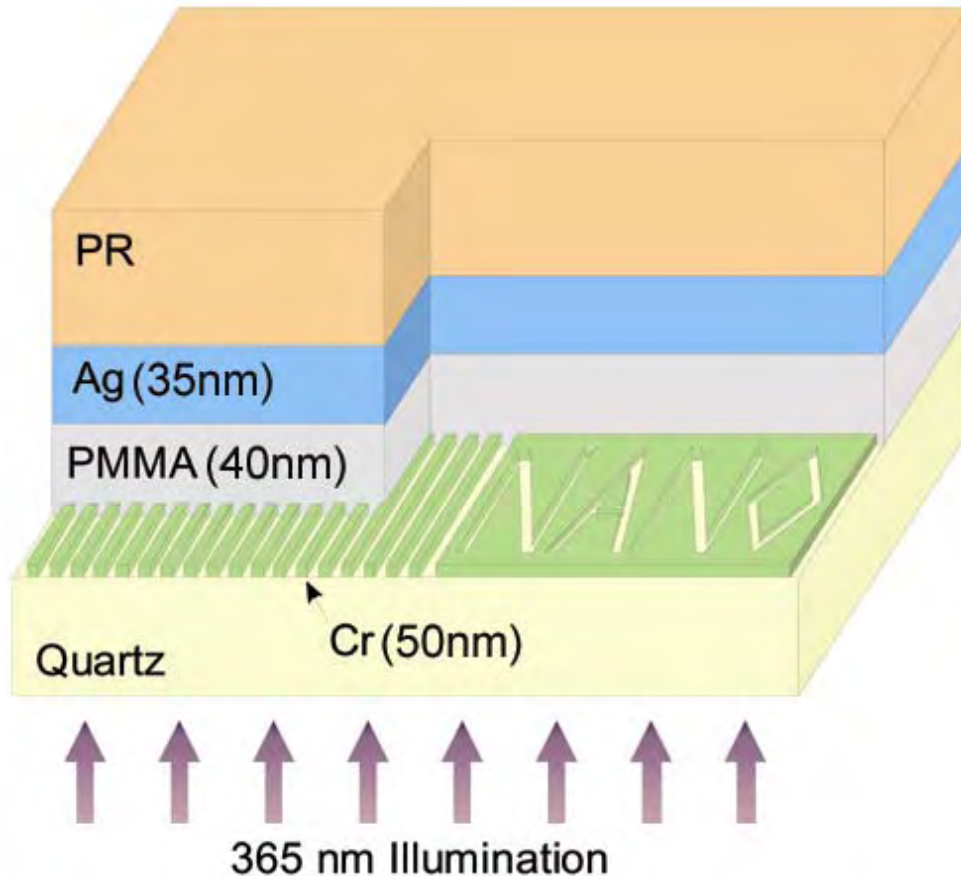
However,



Matching the fields at the boundaries selectively excites a surface plasmon on the far surface.

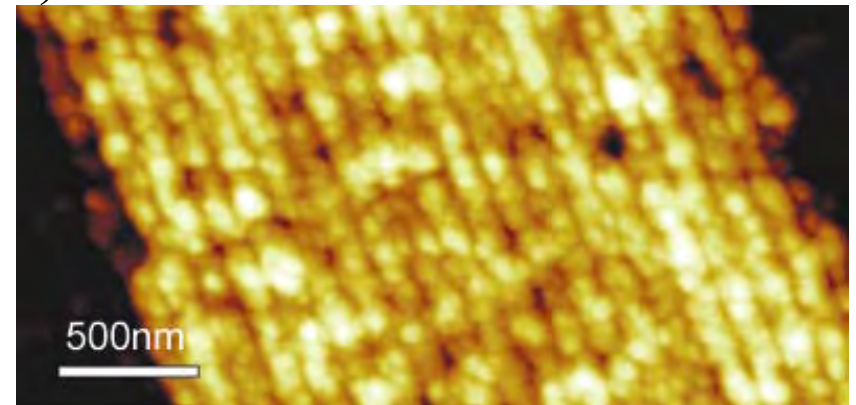
Near field superlensing experiment:

Nicholas Fang, Hyesog Lee, Cheng Sun and Xiang Zhan, UCB



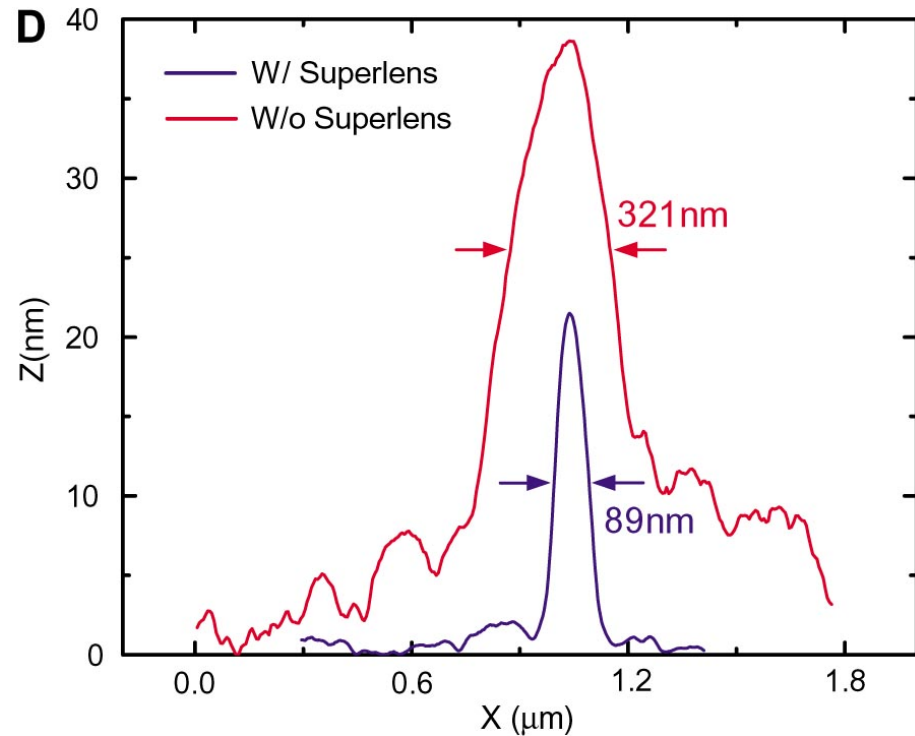
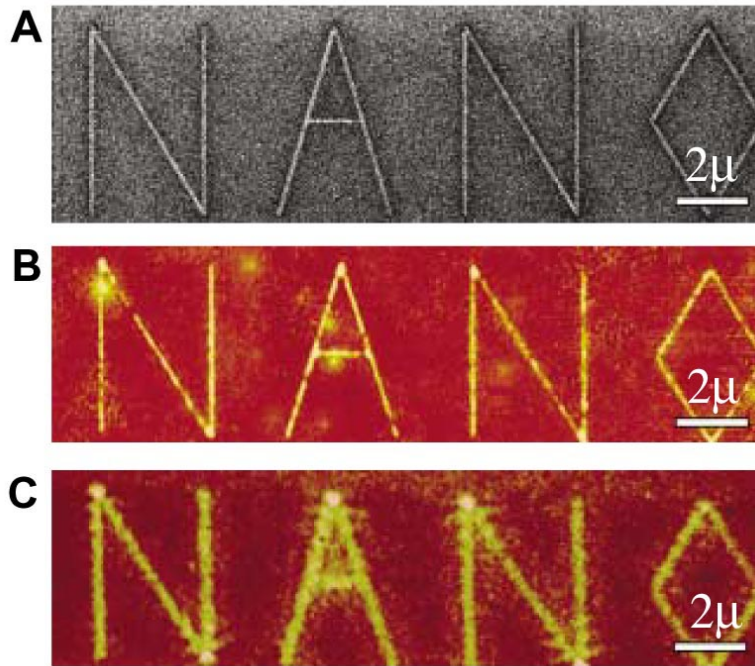
Left: the objects to be imaged are inscribed onto the chrome. Left is an array of 60nm wide slots of 120nm pitch. The image is recorded in the photoresist placed on another side of silver superlens.

Below: Atomic force microscopy of a developed image. This clearly shows a superlens imaging of a 60 nm object ($\lambda/6$).



Imaging by a Silver Superlens.

Nicholas Fang, Hyesog Lee, Cheng Sun, Xiang Zhang, *Science* 534 308 (2005)

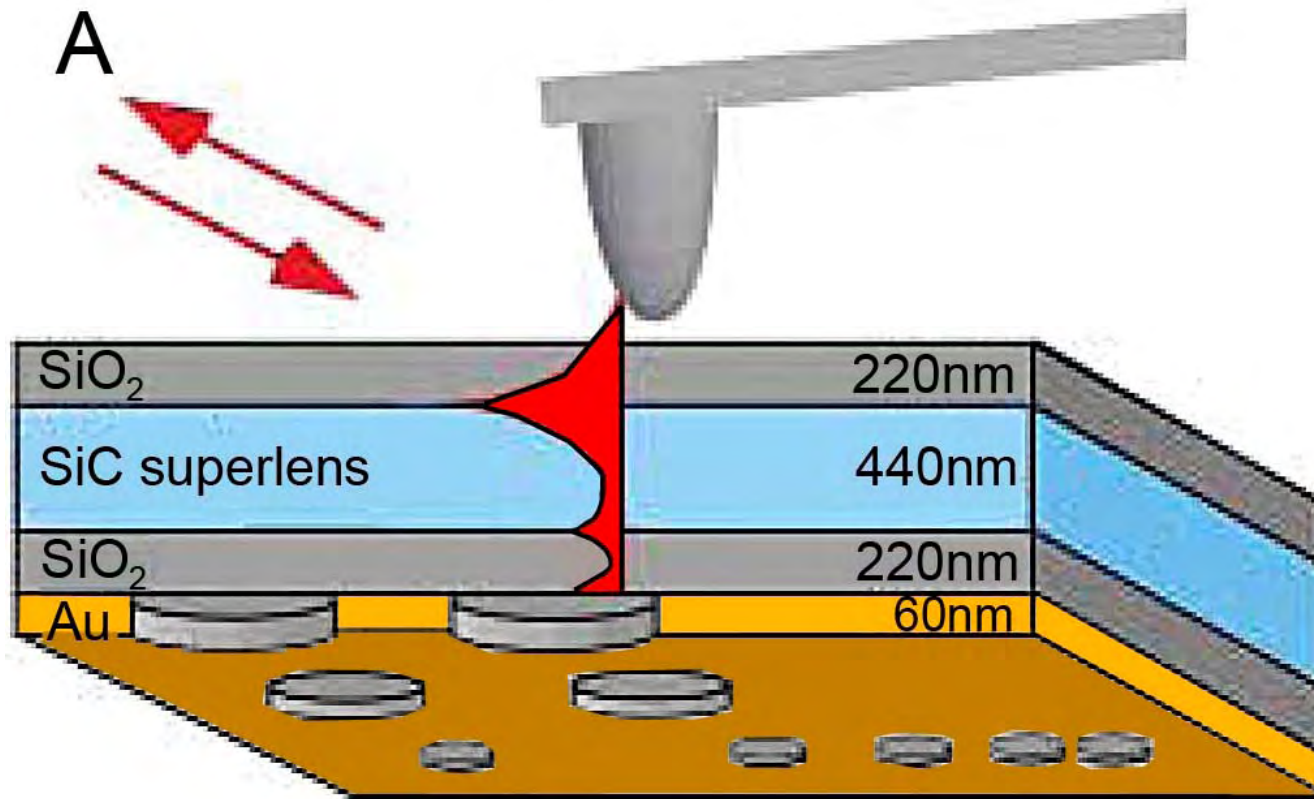


- (A) FIB image of the object. The linewidth of the “NANO” object was 40 nm.
- (B) AFM of the developed image on photoresist with a 35-nm-thick silver superlens.
- (C) AFM of the developed image on photoresist when the layer of silver was replaced by PMMA spacer as a control experiment.
- (D) *blue line*: averaged cross section of letter “A” line width 89nm
red line: control experiment line width 321nm.

Near-Field Microscopy Through a SiC Superlens

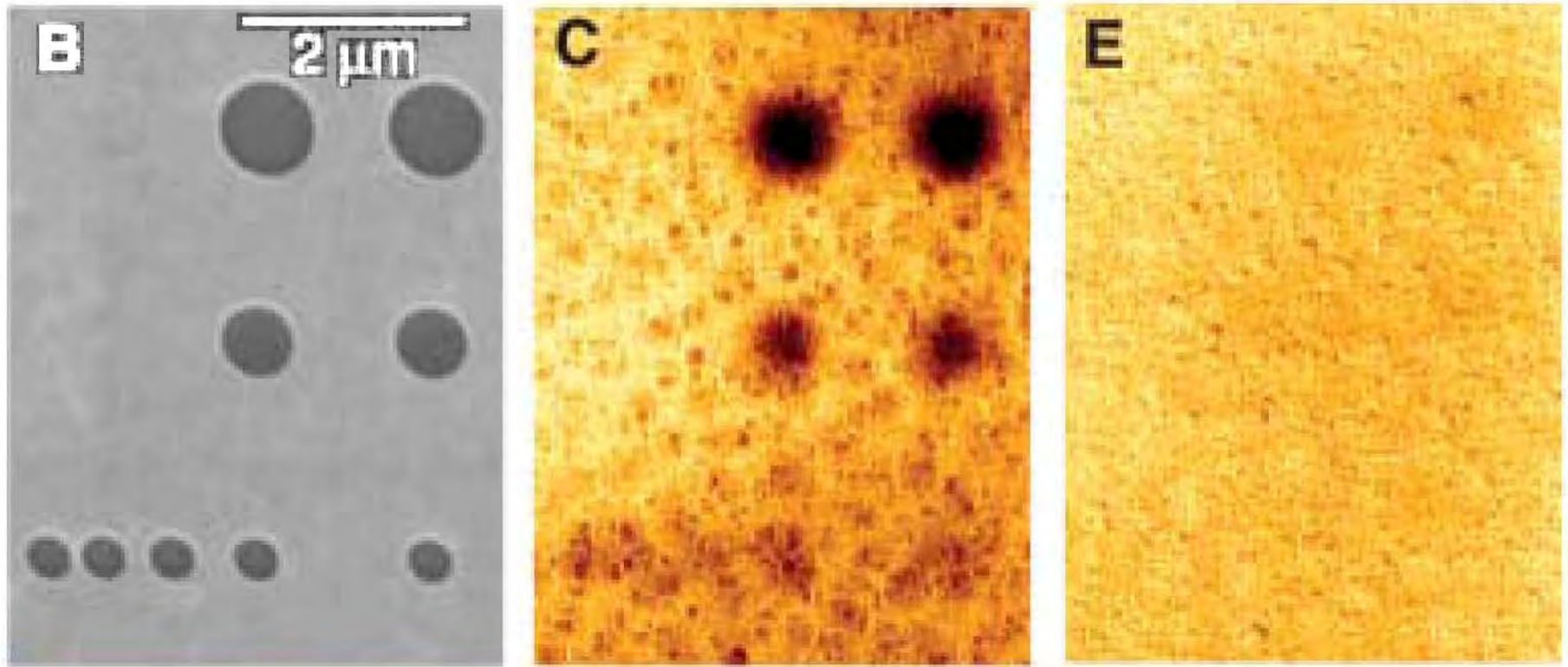
Science, **313** 1595 (2006)

Thomas Taubner, Dmitriy Korobkin, Yaroslav Urzhumov, Gennady Shvets, Rainer Hillenbrand



Near-field microscopy through a 880nm thick superlens structure: the superlens is a 440-nm-thick single-crystalline SiC membrane coated on both sides with 220-nm-thick SiO₂ layers. The two surfaces of the sandwich correspond to the object and the image planes of the lens, respectively. The object plane is covered by a Au film patterned with holes of different diameters

SiC Superlens: the Image



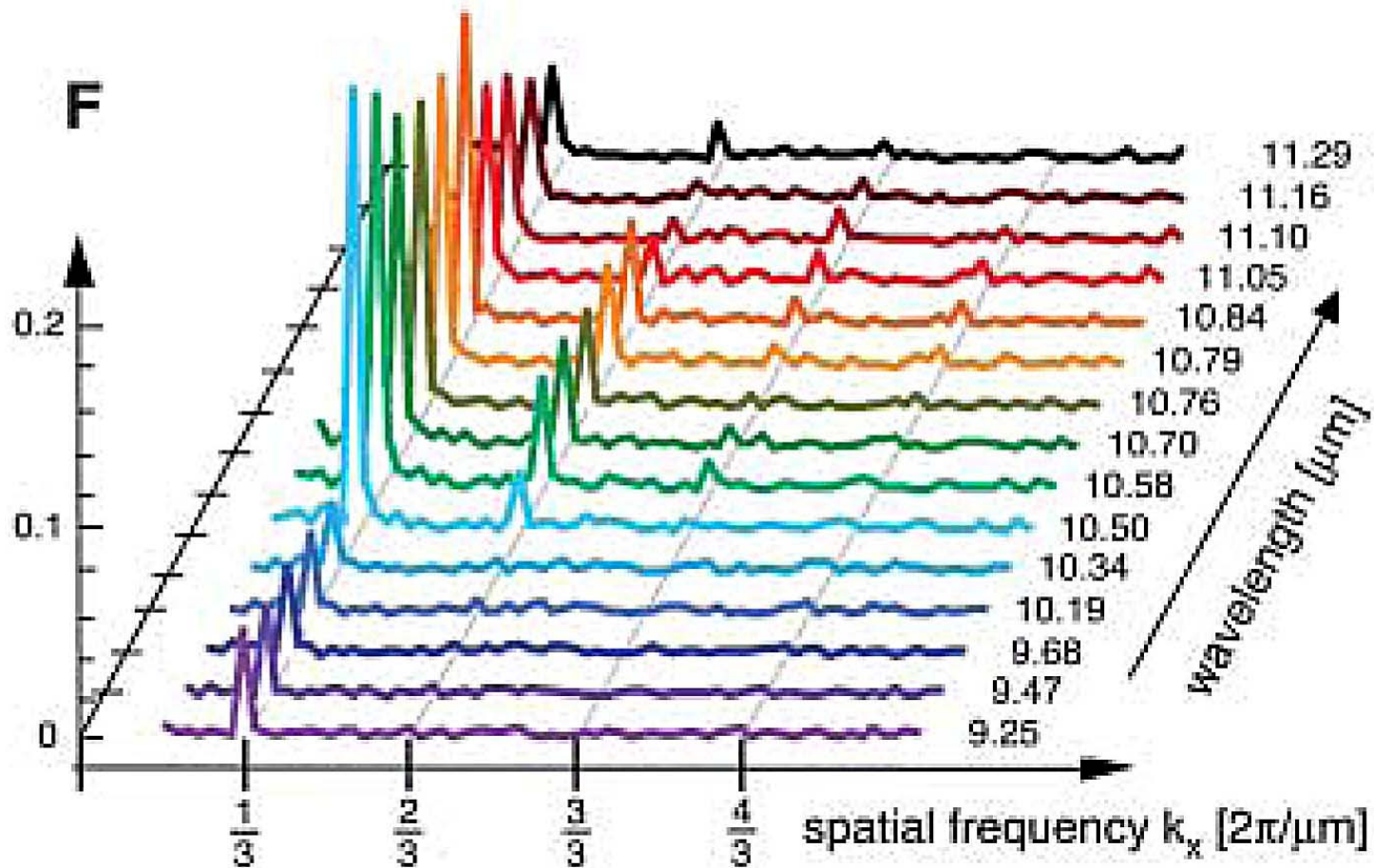
(B) Scanning electron microscope image of the object plane showing holes in a 60nm thick Au film.

(C) amplitude in the image plane at $\lambda = 10.85\mu$ where imaging is expected. NB the permittivity changes with frequency and hence imaging conditions are precisely met only at one frequency.

(E) Control image at $\lambda = 9.25\mu$ (no superlensing)

SiC Superlens:

Fourier transforms of line scans taken from images of a grating, $\lambda \approx 3\mu$ period



High spatial frequencies, up to the grating's fourth harmonic, are imaged by the superlens around $\lambda \approx 10.84\mu$ where the SiC permittivity meets the superlensing condition.

Formal theory: A. J. Ward and J.B. Pendry, *J Mod Op*, **43** 773 (1996)

also D.M. Shyroki (2003)

<http://arxiv.org/abs/physics/0307029v1>

New coordinates in terms of the old: $x'^{j'}(x^j)$

In the new coordinate system we must use renormalized values of the permittivity and permeability, ϵ, μ :

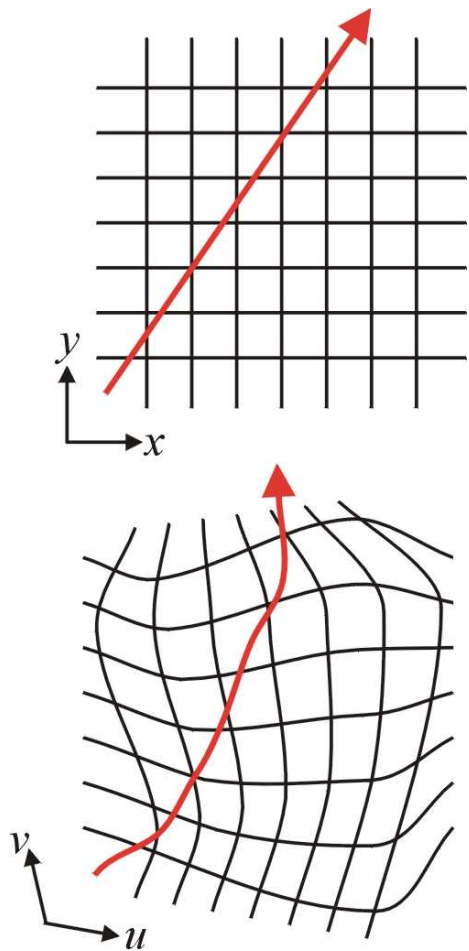
$$\epsilon'^{i'j'} = [\det(\Lambda)]^{-1} \Lambda_i^{i'} \Lambda_j^{j'} \epsilon^{ij}$$

$$\mu'^{i'j'} = [\det(\Lambda)]^{-1} \Lambda_i^{i'} \Lambda_j^{j'} \mu^{ij}$$

where,

$$\Lambda_j^{j'} = \frac{\partial x'^{j'}}{\partial x^j}$$

For the special case of conformal transformations in 2D systems, ϵ, μ are unchanged.



Top: a ray in free space with the background Cartesian coordinate grid shown.

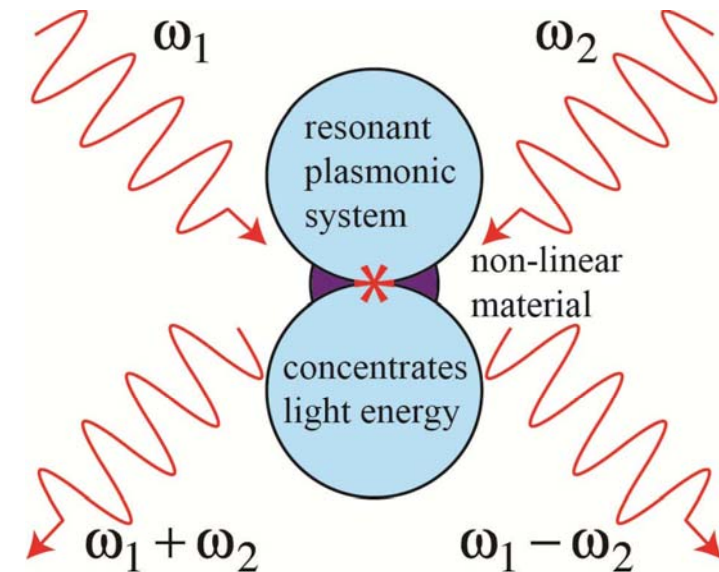
Bottom: the distorted ray trajectory with distorted coordinates.

Singular plasmonic structures

Metal surfaces support *surface plasmons* whose properties depend critically on the shape of the surface. In particular singularities such as sharp points, or touching points of two surfaces attract a high density of modes. These can be exploited to capture and concentrate photons into nanometric areas.

Transformation optics provides unique insight into these processes:

- relates the spectra of many different singular structures to a single ‘mother’ structure.
- reveals ‘hidden symmetries not apparent in the original structure
- hence enables analytic solutions for the fields
- gives a detailed understanding of field enhancements, Van der Waals forces, and near-field heat transfer



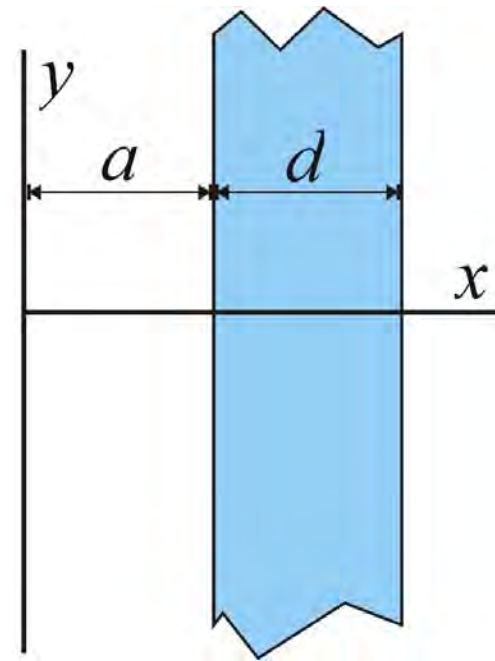
In this talk we shall work in the extreme near field limit, assuming length scales much less than the wavelength, where the quasistatic approximation is valid.

Constructing a broadband absorber

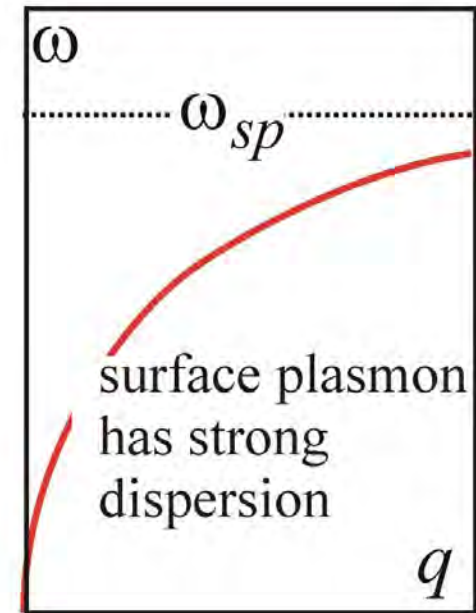
Resonant systems, such as silver spheres, enhance the absorption of radiation hence greatly improving the sensitivity to adsorbed molecules; but absorption by a single resonance is narrow band and therefore of limited use.

- start with a dipole exciting an infinite system – most infinite systems have a *broadband* continuum
- invert about the origin to convert to a finite system excited by a plane wave. The *spectrum is unchanged and remains broadband*.

a metallic slab of finite thickness has a broadband spectrum

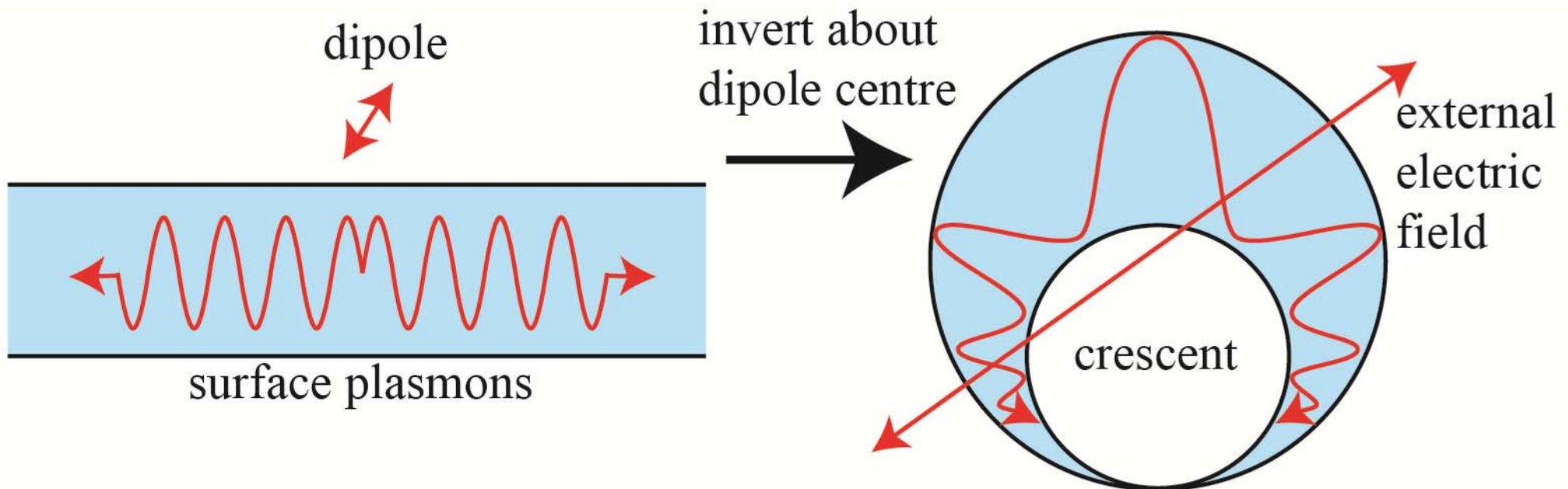


finite slab of silver



Inversion about the origin, $z' = 1/z$, converts a slab to a cylindrical crescent

The dipole source is transformed into a uniform electric field

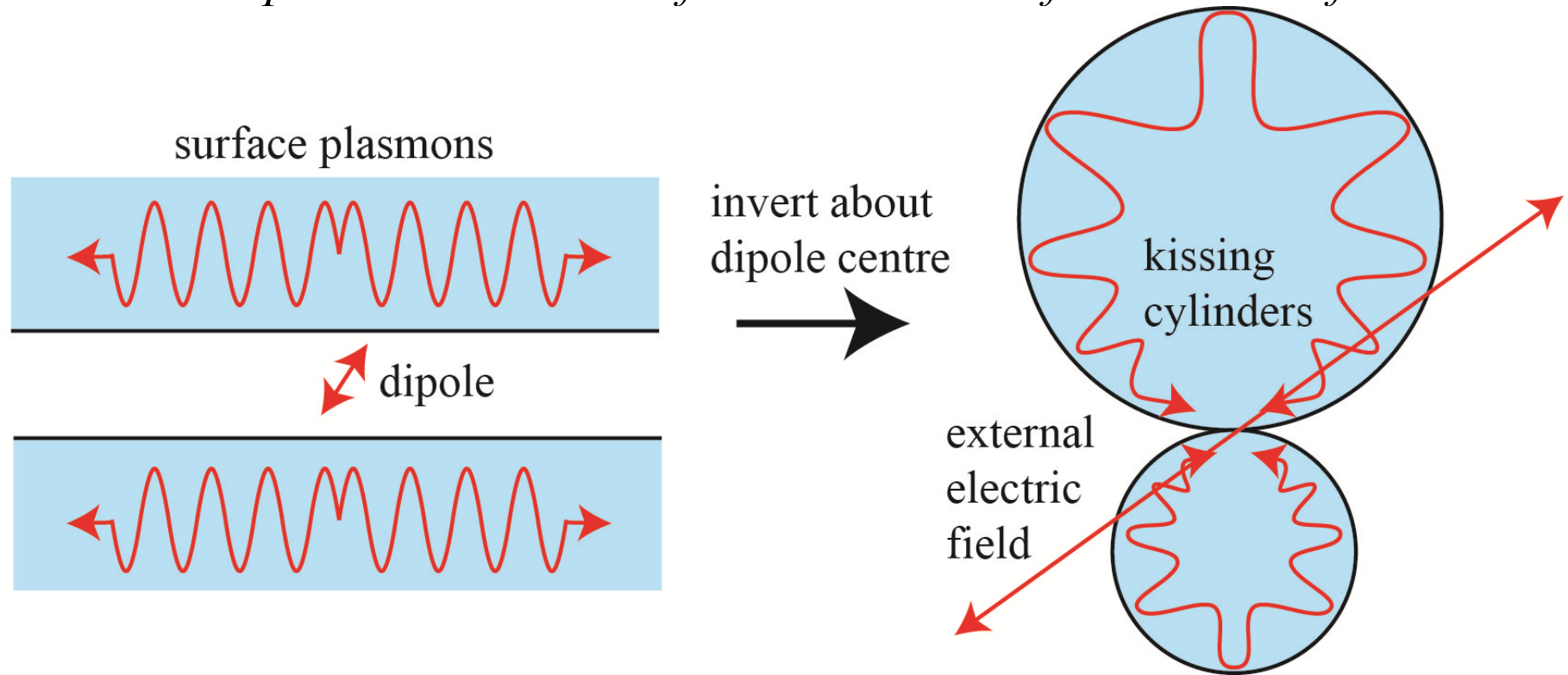


Left: a thin slab of metal supports surface plasmons that couple to a dipole source, transporting its energy to infinity. The spectrum is continuous and broadband therefore the process is effective over a wide range of frequencies.

Right: the transformed material now comprises a cylinder with cross section in the form of a crescent. The dipole source is transformed into a uniform electric field.

Inversion about the origin, $z' = 1/z$, converts a cavity to a pair of kissing cylinders

The dipole source is transformed into a uniform electric field

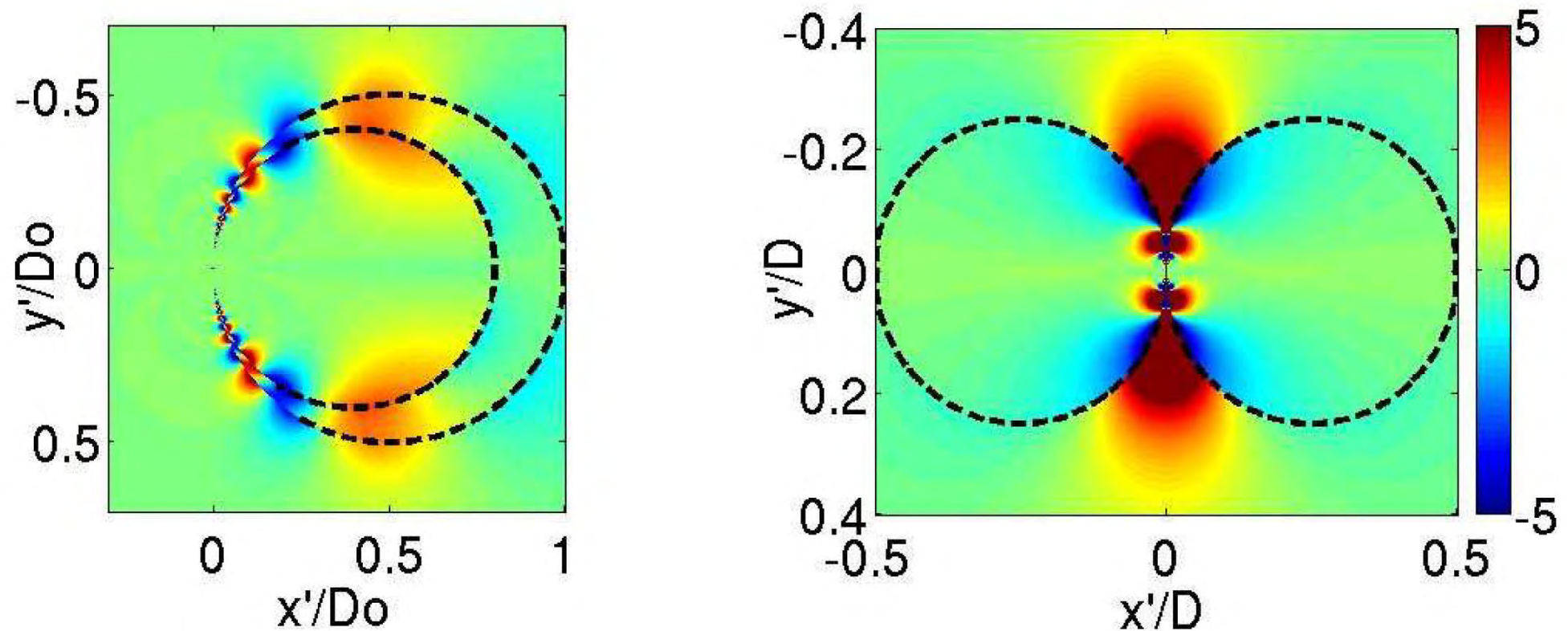


Left: a cavity supports surface plasmons that couple to a dipole source, transporting its energy to infinity. The spectrum is continuous.

Right: the transformed material now comprises two kissing cylinders. The dipole source is transformed into a uniform electric field.

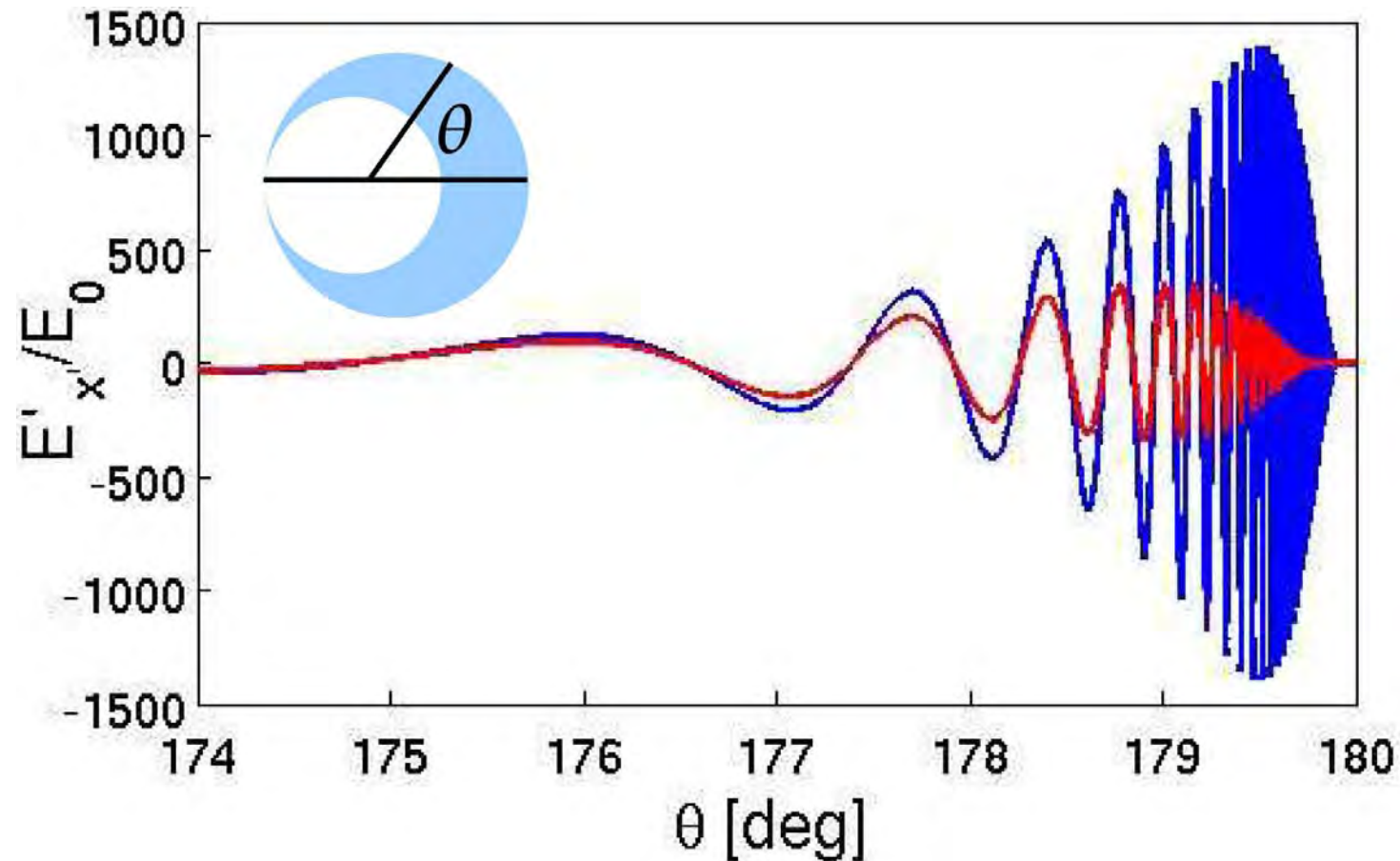
Broadband field enhancement in singular structures

(Alexandre Aubry, Dang Yuan Lei, Antonio I. Fernandez-Dominguez, et al.)



Calculated E_x normalized to the incoming field (E -field along x). The left and right panels display the field in the crescent and in the two kissing cylinders respectively. The metal is silver and $\omega = 0.9\omega_{sp}$. The scale is restricted to -10^5 to $+10^5$ but note that the field magnitude is far larger around the structural singularities.

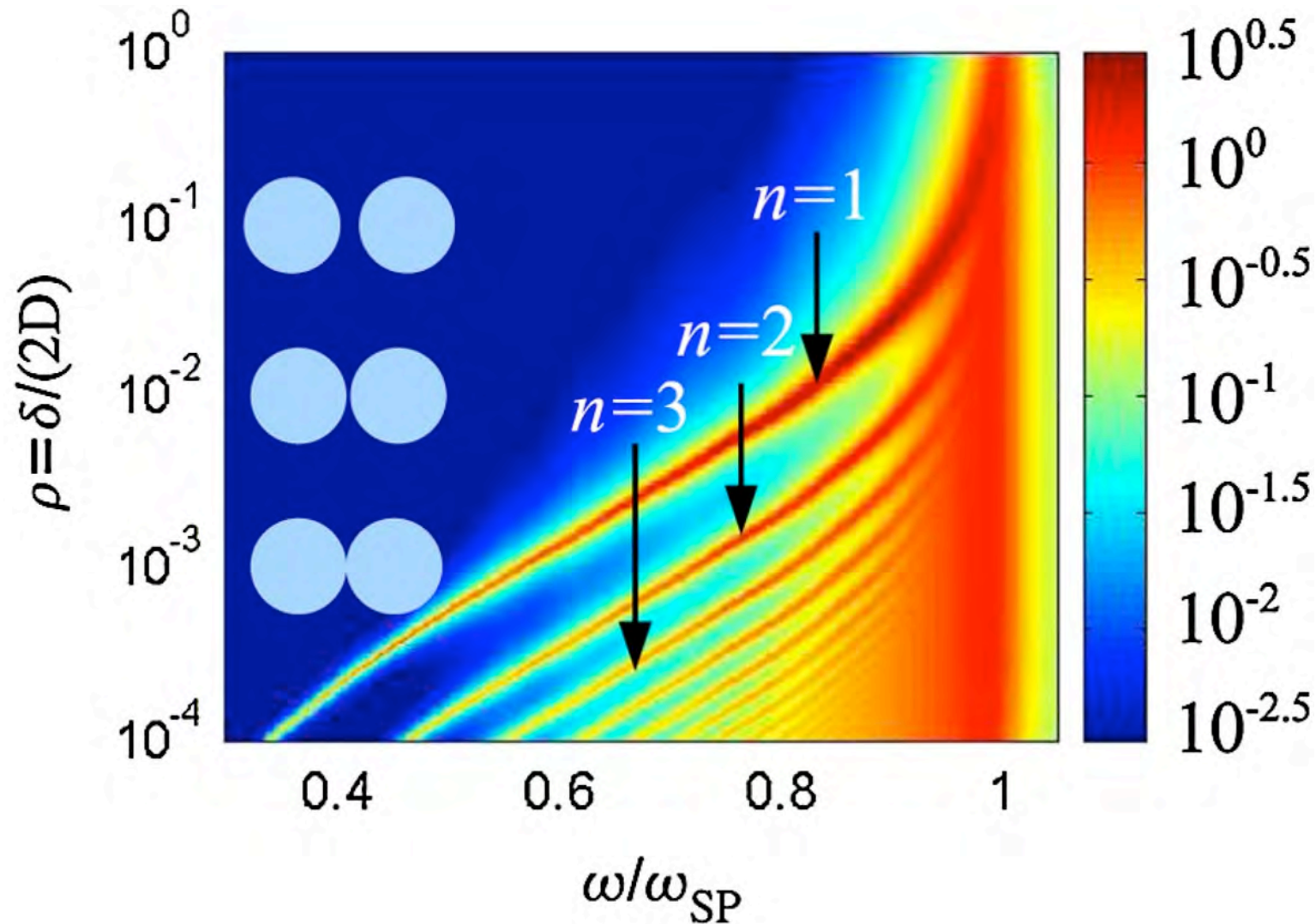
Field enhancement versus angle – crescent



Blue curve: E_x at the surface of the crescent, plotted as a function of θ , for $\omega = 0.75\omega_{sp}$ and $\varepsilon = -7.058 + 0.213i$ taken from Johnson and Christy.

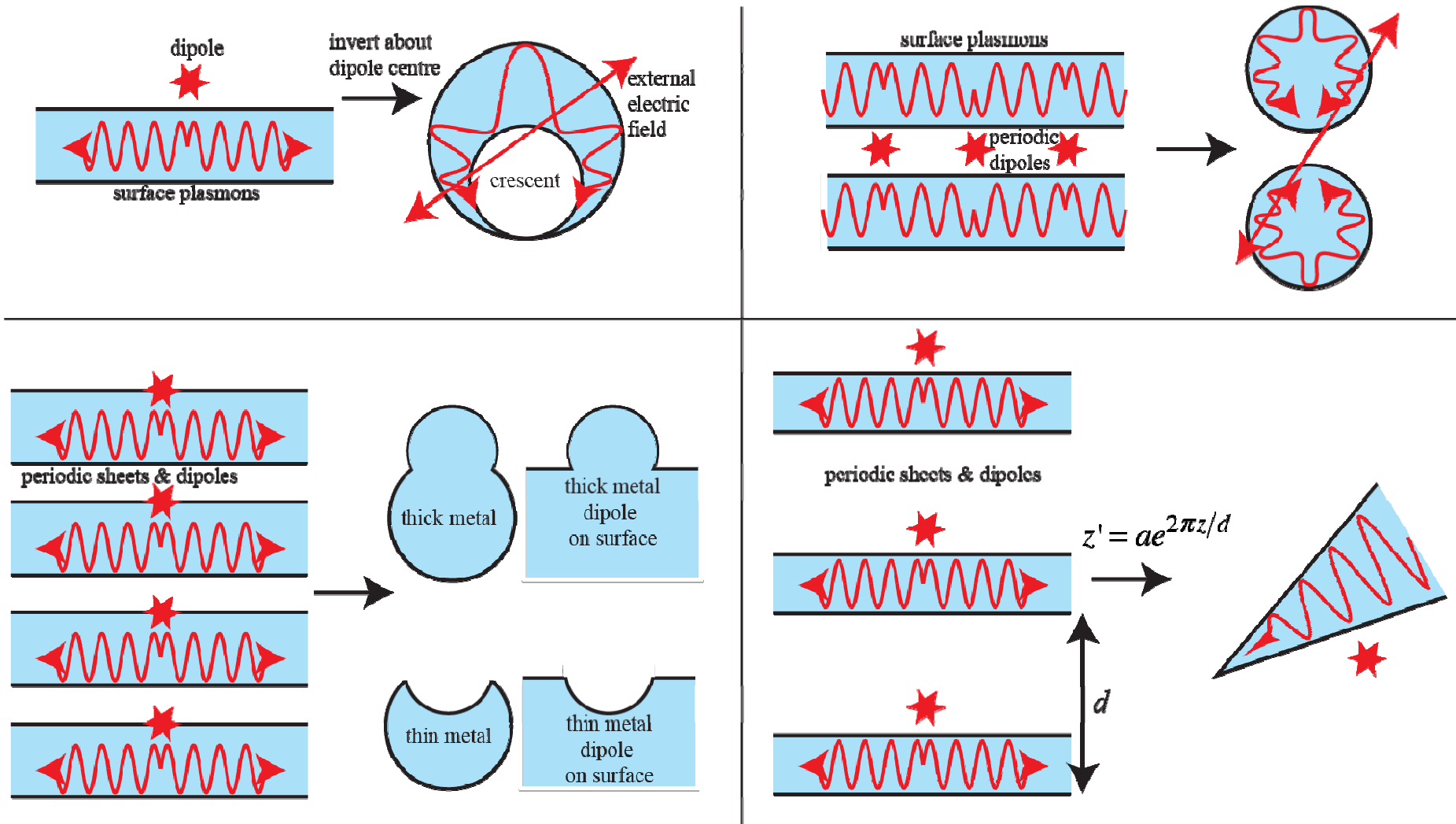
Red curve: $\varepsilon = -7.058 + 2 \times 0.213i$ i.e. more loss. Both curves are normalised to the incoming field amplitude E_0 . The crescent is defined by the ratio of diameters $r = 0.5$

Absorption cross section: non-touching cylinders



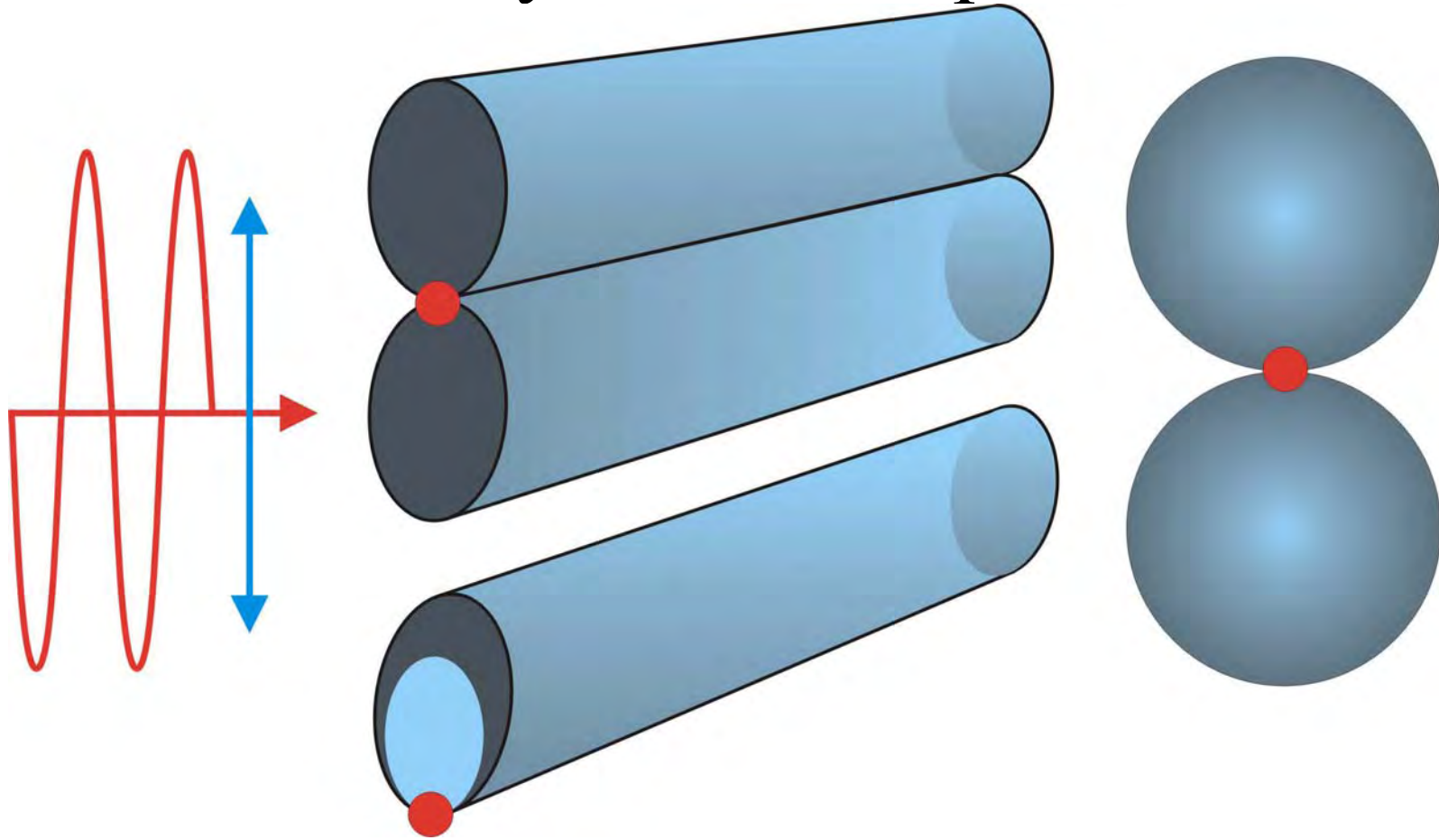
Absorption cross section normalised to the physical cross section, D_0 , as a function of separation between the cylinders, δ .

Plasmonic Zoo



Most of the well known singular structures can be related by a transformation to a common ‘mother structure’ whose solution is to be had analytically. see: Y. Luo et al., “Surface Plasmons and Singularities”, *Nano Letters*, **10** 4186-4191 (2010).

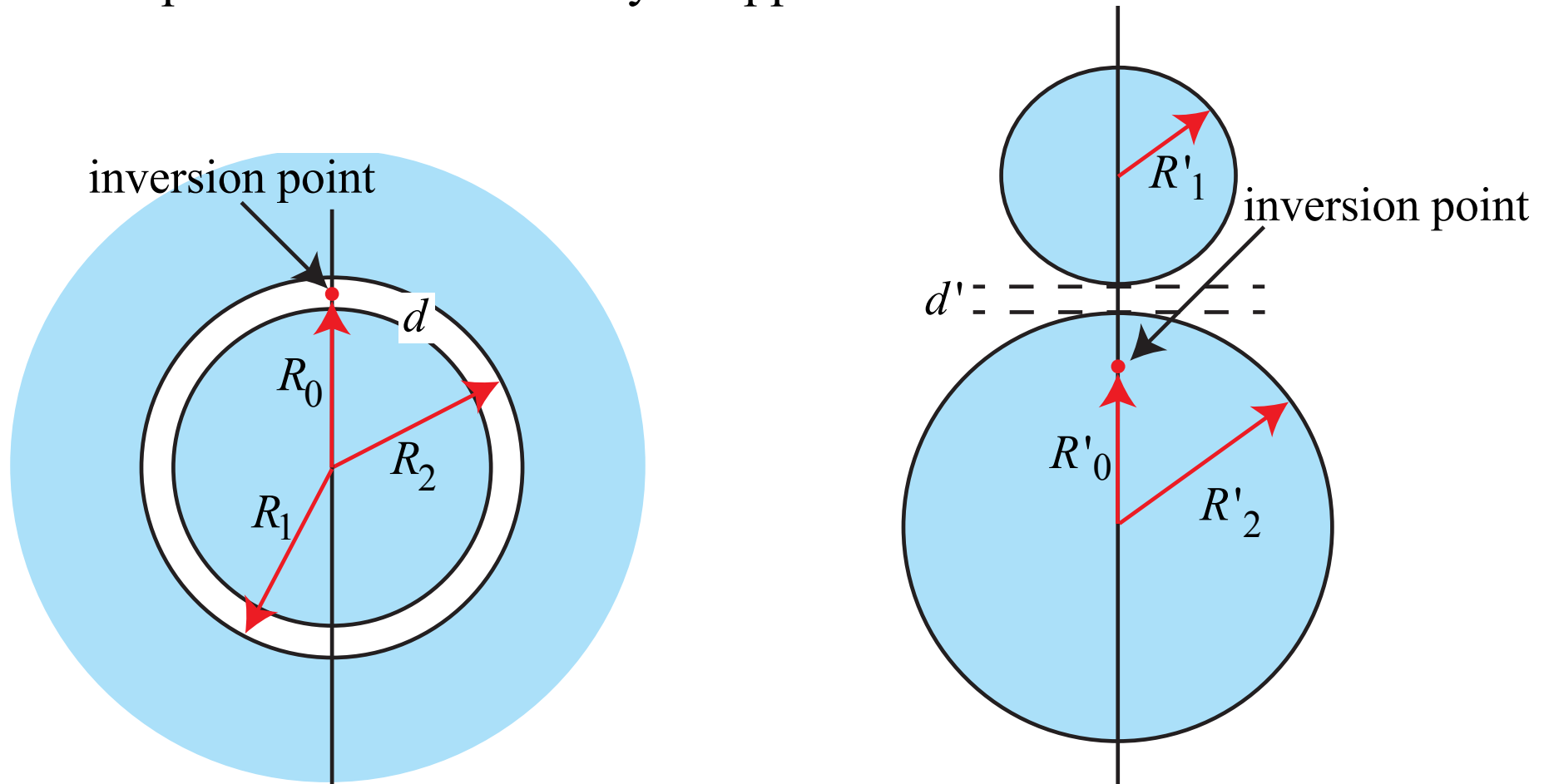
Extension of Harvesting Theory from Cylinders to Spheres



Analytic theory in the electrostatic limit is exact for touching cylinders. For spheres theory approximates to the cylindrical solution near the touching point.

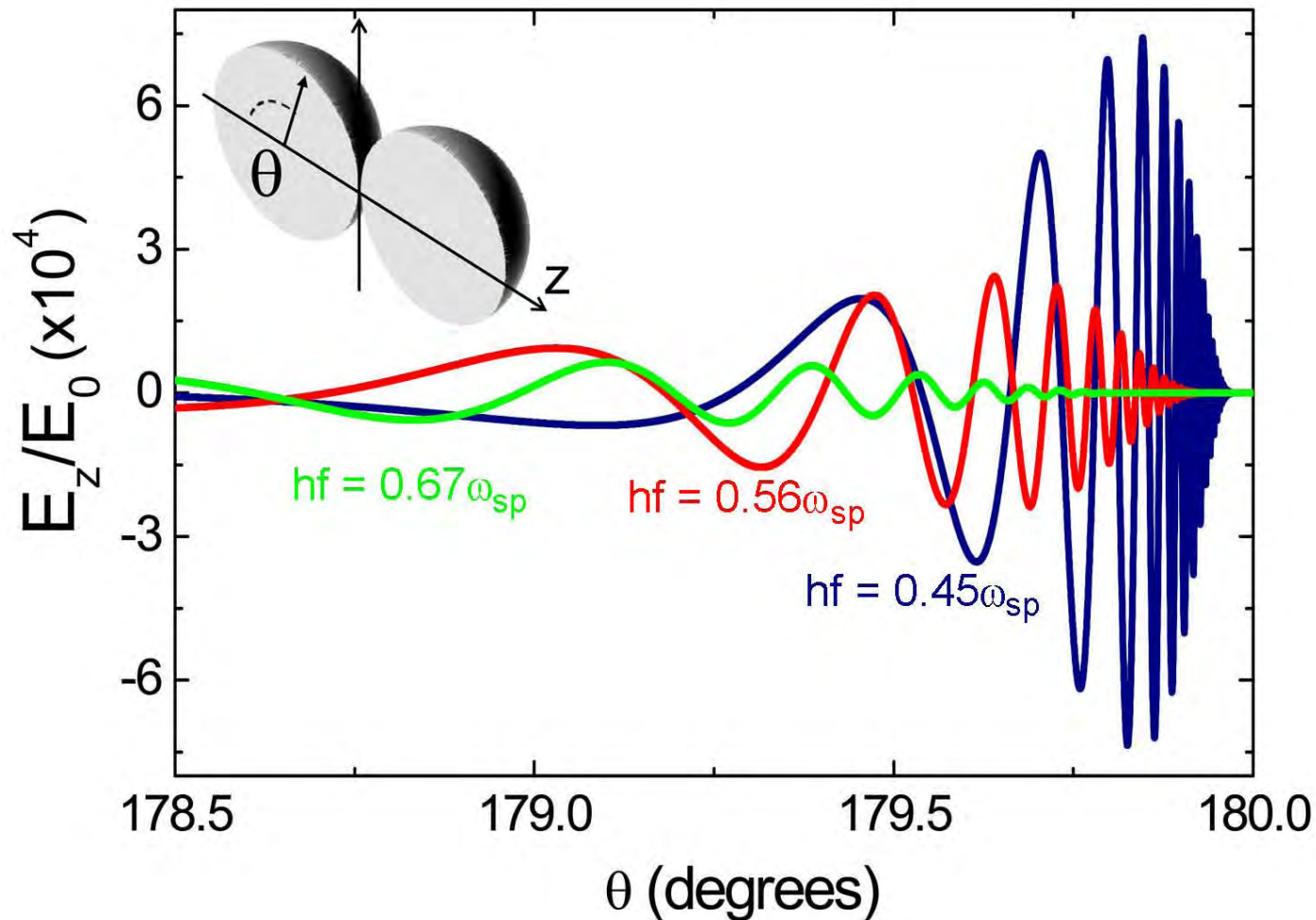
Extension to 3D – two spheres

Applying an inversion to the spherical annulus structure on the left leads to two separated spheres shown on the right. Solutions in the left hand geometry are much simpler and accurate analytic approximations can be made.



Spheres as Light Harvesting Devices

Theory by Antonio Fernandez-Dominguez



Electric field enhancement at various photon frequencies for touching spheres. Enhancement is an order of magnitude greater than for touching cylinders because energy is compressed in 2 directions.

What can go wrong?

The theory predicts spectacular enhancements in the harvested fields, even when realistic values of the silver permittivity are included. **Harvesting is much less sensitive to resistive losses than is perfect imaging.**

Enhancements in field strength of 10^4 are predicted, implying an enhancement of the SERS signal of 10^{16} . Several factors will prevent this ideal from being attained:

- radiative losses
- problems in nm scale precision manufacture
- non locality of ϵ

Nevertheless substantial effects can be expected

Radiative Losses

In the electrostatic approximation there are no radiative losses. This is a valid assumption provided that the cylinders are small compared to the wavelength.

In practice this means:

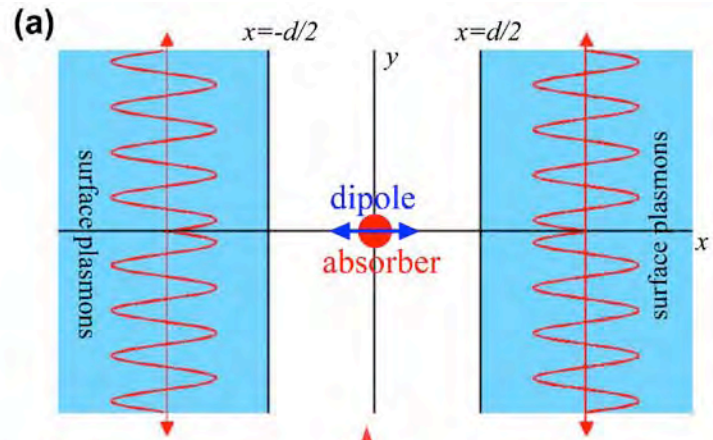
$$D(\text{diameter}) < 200\text{nm}$$

Their effect is to damp the resonant harvesting states and steal energy from the light harvesting mechanism.

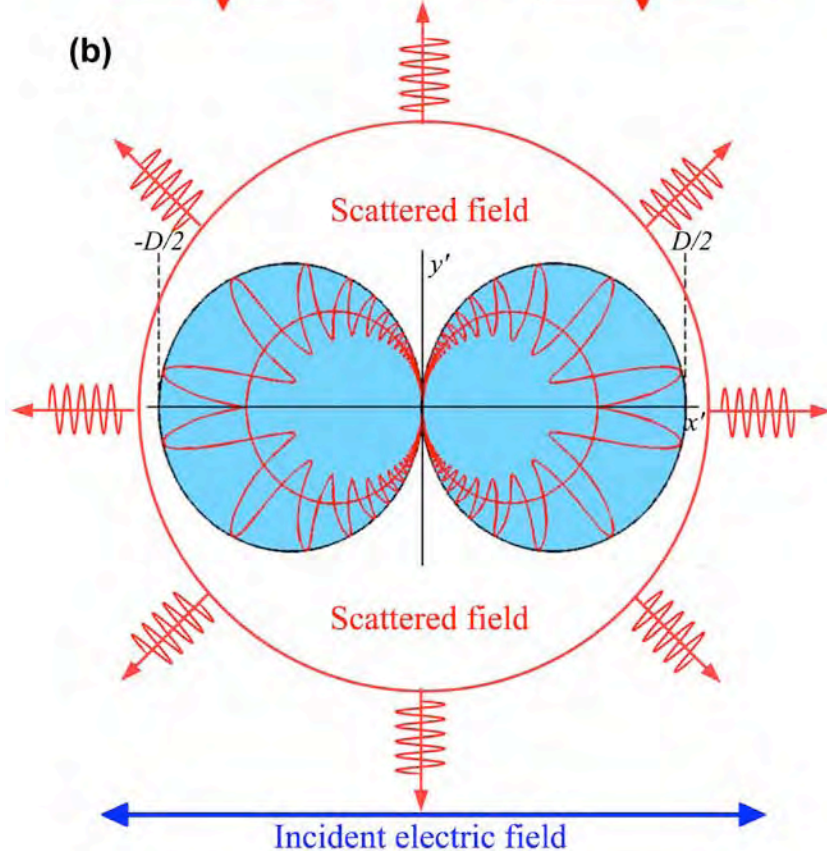
In the electrostatic limit the harvesting cross section $\sigma_a \propto D^2$ reflecting the scale invariance of an electrostatic system.

However computer simulations using COMSOL show this scaling breaking down as radiative corrections kick in and σ_a falling dramatically.

Calculating radiative corrections analytically



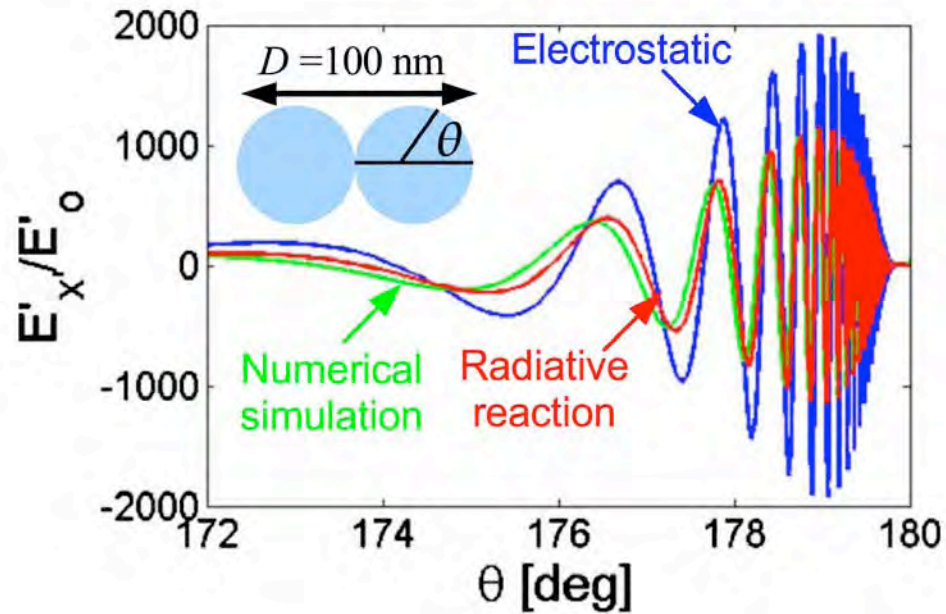
(a) Two semi-infinite metal slabs support surface plasmons that couple to a dipole source, transporting its energy to infinity.



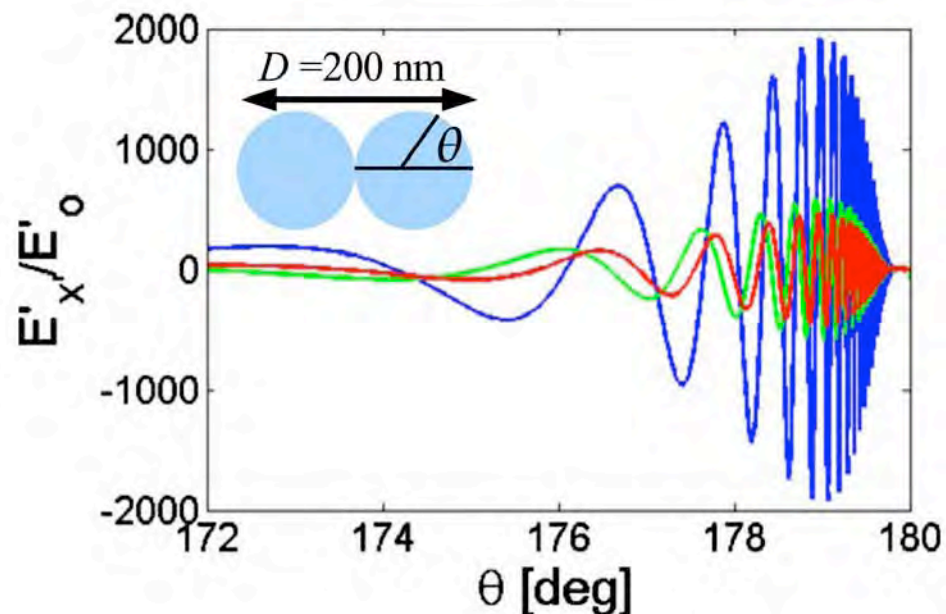
A fictional absorbing particle superimposed on the emitting dipole is chosen to account for the radiative damping in the transformed geometry.

(b) The transformed material consists of two kissing cylinders. The dipole source is transformed into a uniform electric field, and the radiative losses are approximated by lossy material outside the large sphere.

The effect of radiative loss on enhancement



Electric field along the x - direction normalized by the incident electric field E_0 , for $D = 100$ nm and $D = 200$ nm for $\omega = 0.9 \omega_{sp}$.



The analytical prediction for the effect of radiative loss (red) is compared to the numerical result (green) and to the electrostatic case where there is no radiative loss (blue).

Nonlocality – what is it?

Formal definition: the longitudinal permittivity, ε_L , depends on wave vector as well as frequency.

The *physical interpretation* for metals at optical frequencies is that the bulk plasmon frequency also depends on wave vector and is defined by,

$$\varepsilon_L(k, \omega_p) = \varepsilon_\infty \left[1 - \frac{\omega_0^2}{\omega_p(\omega_p + i\gamma) - \beta^2 k^2} \right] = 0$$

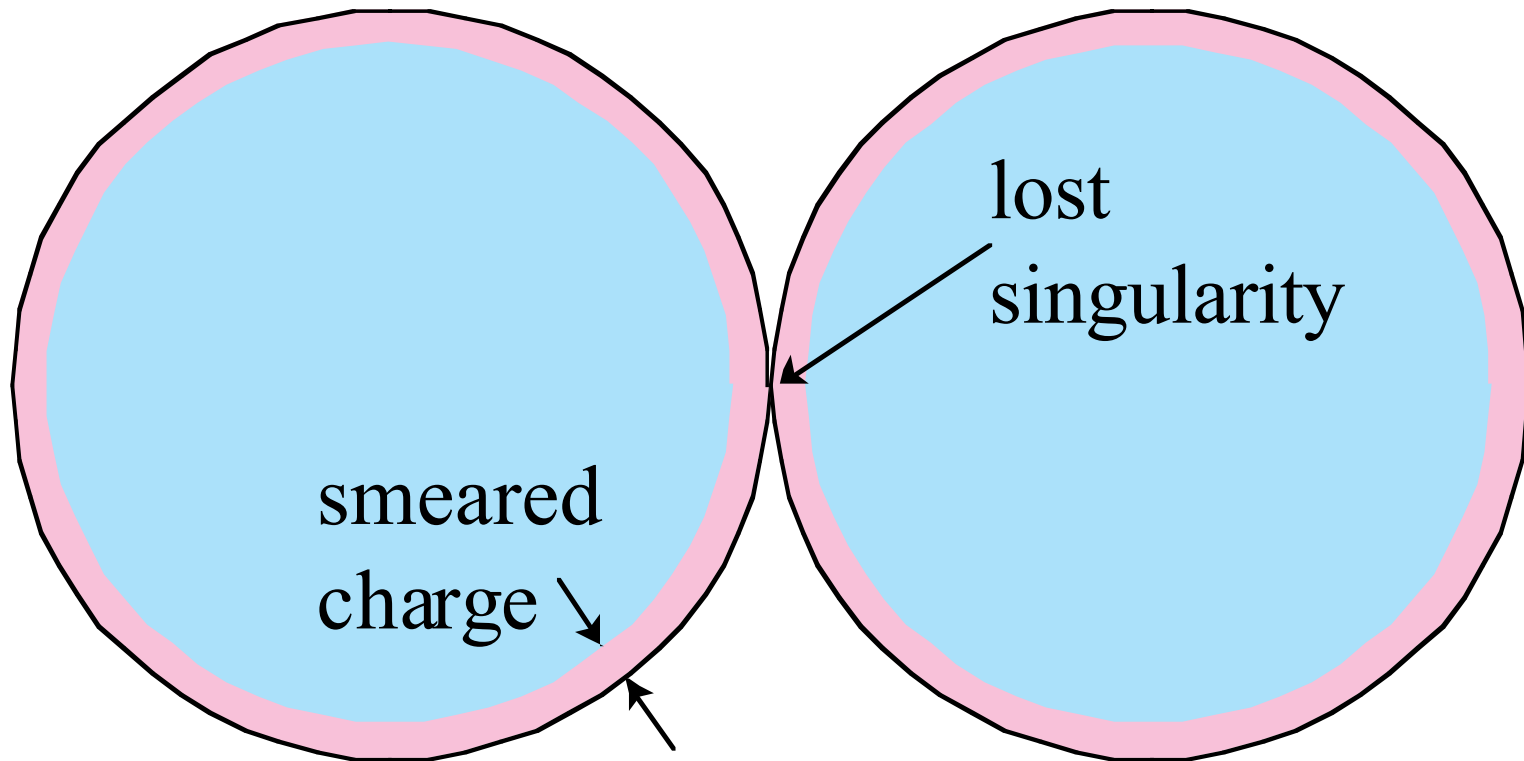
Since the bulk plasmon controls the screening charge in a metal, the surface charges induced by external fields no longer appear as delta functions at the surface but decay smoothly into the bulk with a decay defined by,

$$\exp(-\delta^{-1}z), \quad \delta^{-1} = \beta^{-1} \sqrt{\omega_0^2 - \omega_p(\omega_p + i\gamma)}$$

Typically $\delta \approx 0.2\text{nm}$, a very small length, but one that is sometimes important.

Nonlocality and light harvesting

Nonlocality smears out polarisation charge responsible for driving field enhancements at the touching point. Although the cylinders appear to touch, the charge distributions do not. Hence the field enhancement is degraded.



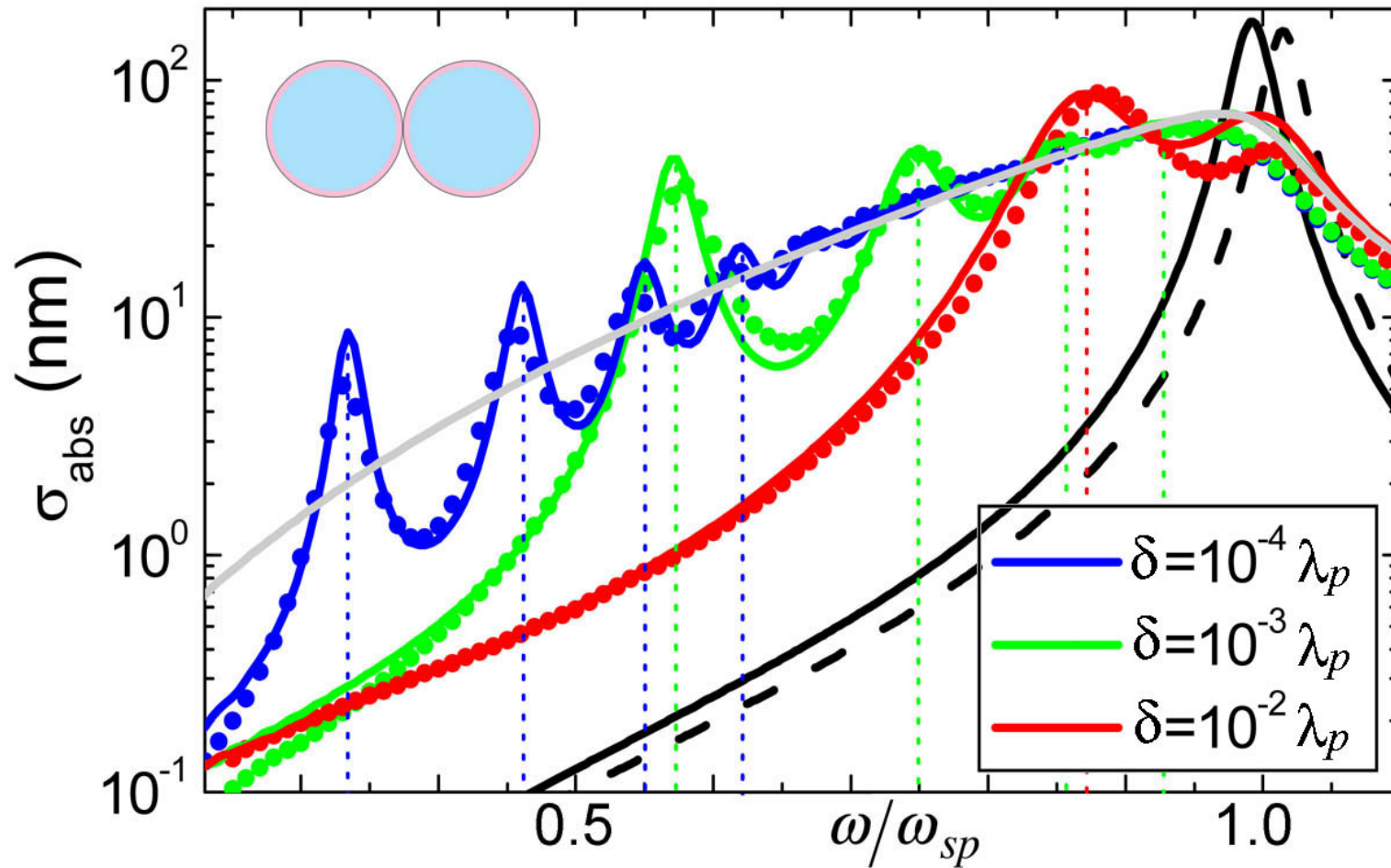
Nonlocality and field enhancement

Because the polarisation charge distributions are smeared, and no longer touch at the singularity, the characteristics of two touching but nonlocal cylinders resemble two almost touching cylinders:

- waves travelling towards the touching points no longer slow to zero velocity, but head on past the touching point and as a result:
- the spectra are no longer continuous
- enhancement is reduced in the vicinity of the touching point

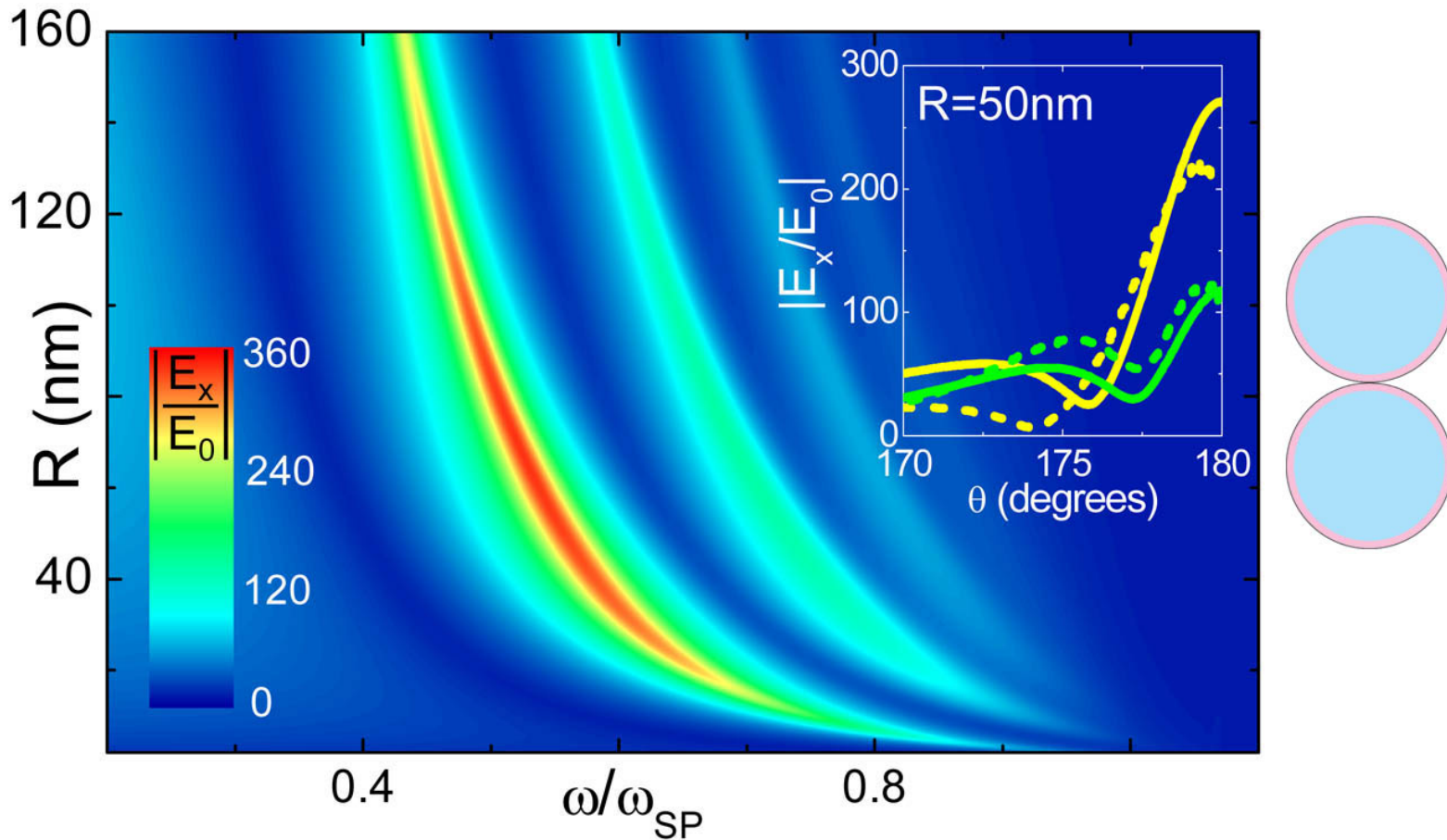
The effects grow larger as the overall size of the system shrinks

Nonlocality quantises spectra of touching cylinders



Absorption spectra for 10nm radii non-local cylinders for several degrees of nonlocality. The green line shows a typical result. The local approximation is shown in grey. Black line: results for a single cylinder.

Nonlocality versus radiation loss



Electric field enhancement for two touching cylinders at the touching point as a function of cylinder radius, R , and frequency ω . **Radiation loss** kills enhancement for large cylinders, **non local effects** for small. Optimum enhancement is found for $35\text{nm} < R < 80\text{nm}$.

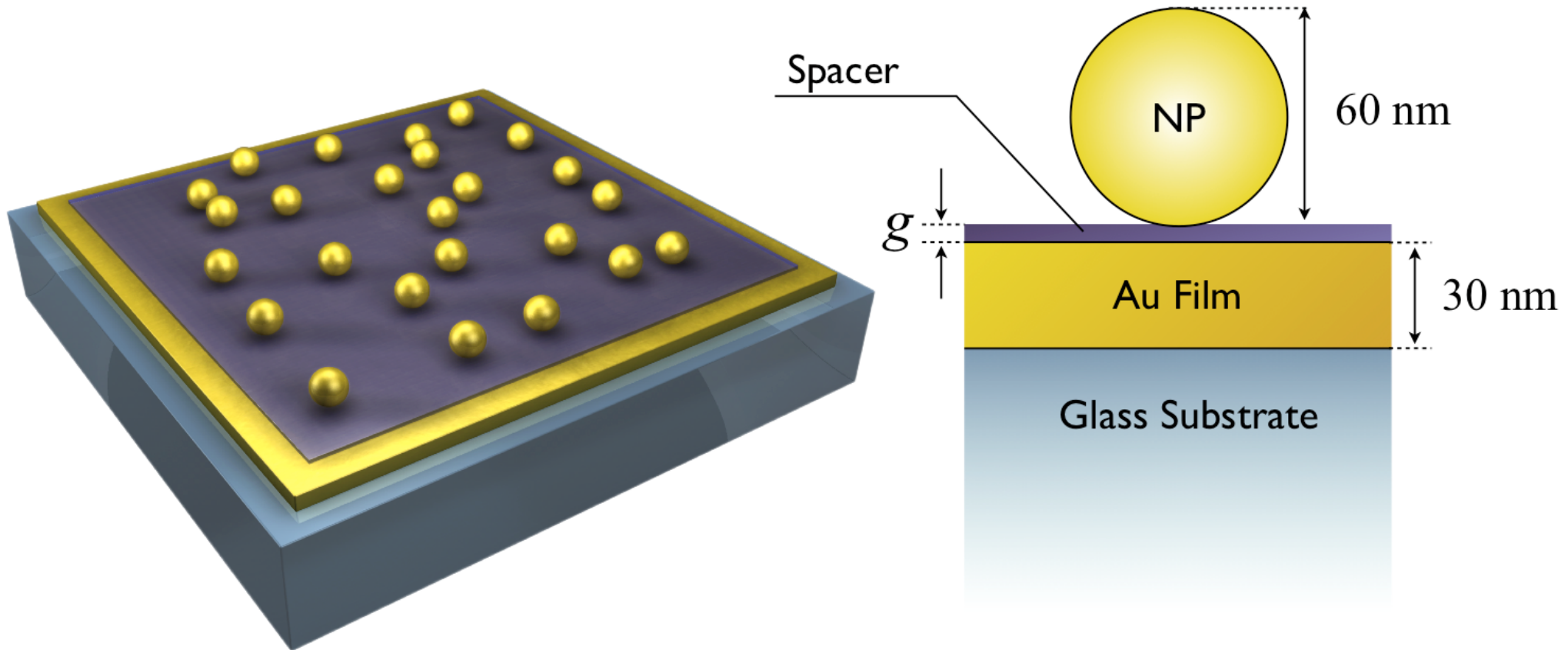
Measuring non-locality

reported in:

Probing the Ultimate Limits of Plasmonic Enhancement

C. Ciraci, R. T. Hill, J. J. Mock, Y. Urzhumov, A. I. Fernández-Domínguez,
S. A. Maier, J. B. Pendry, A. Chilkoti and D. R. Smith,
Science, **337**, 1071-4, 2012

Measuring non-locality – experimental setup

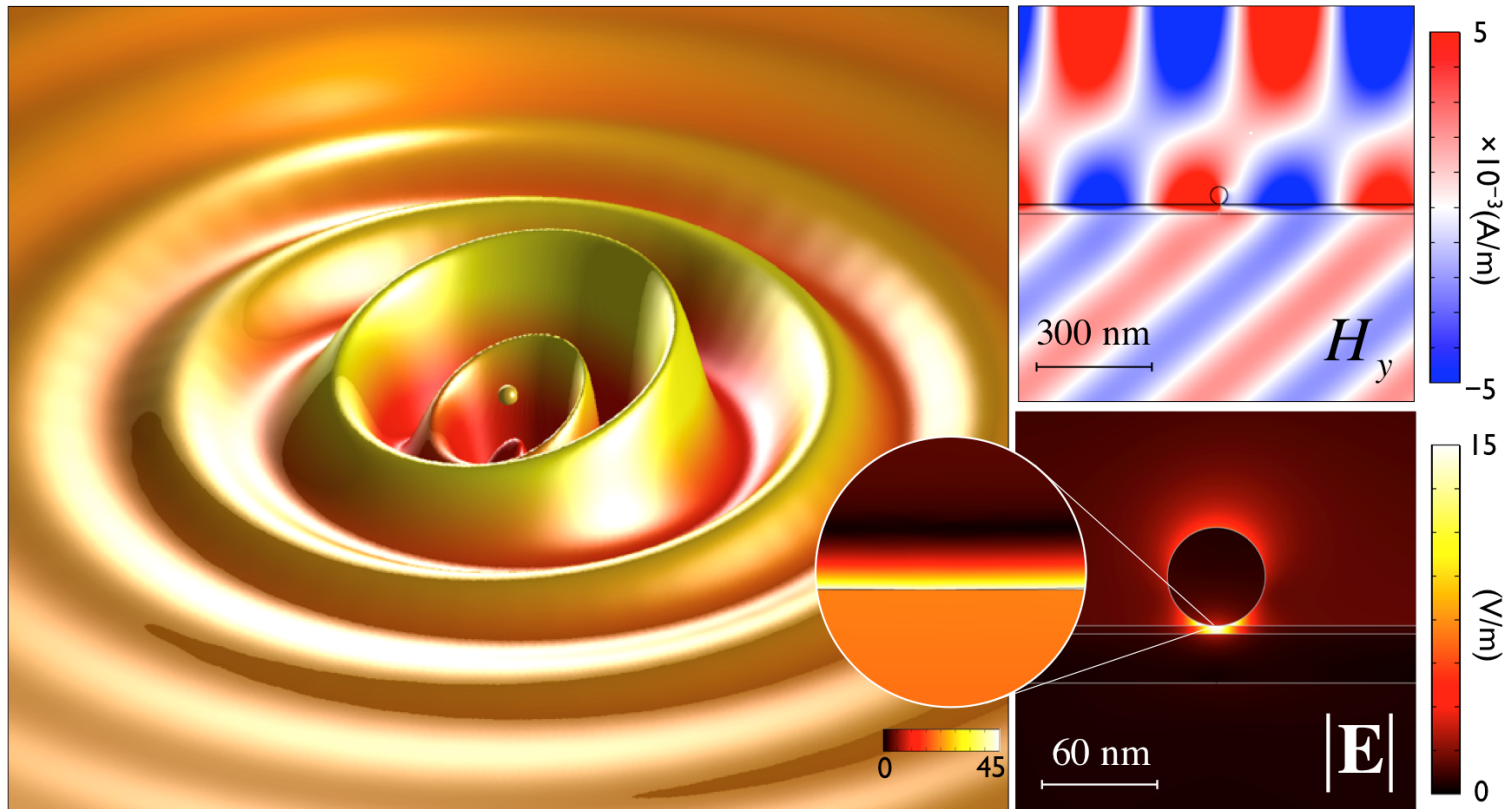


Geometry of the film-coupled nanoparticle.

Left: Schematic of the sample.

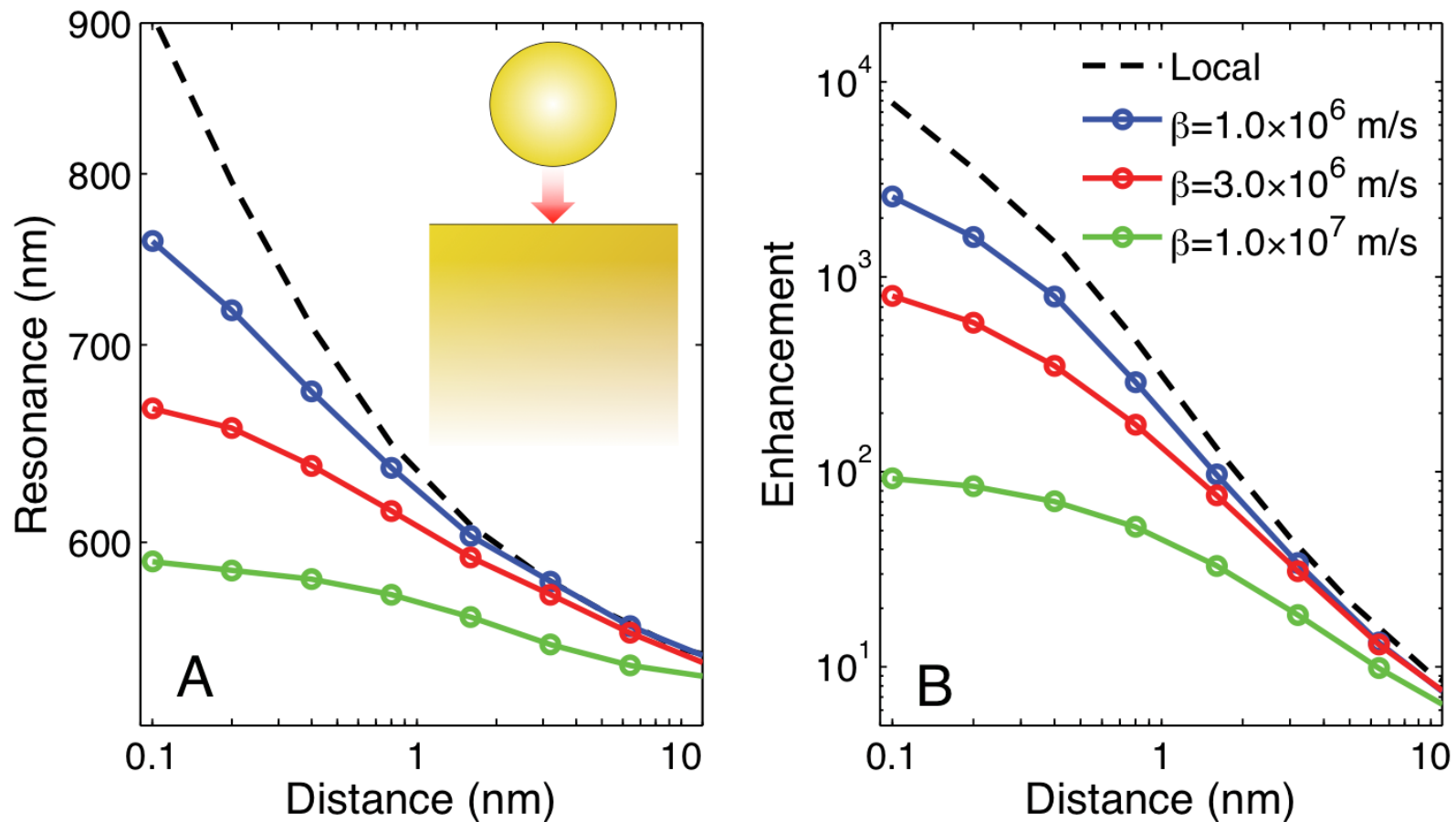
Right: Cross-section of a single film-coupled nanosphere.

Measuring non-locality – simulations I



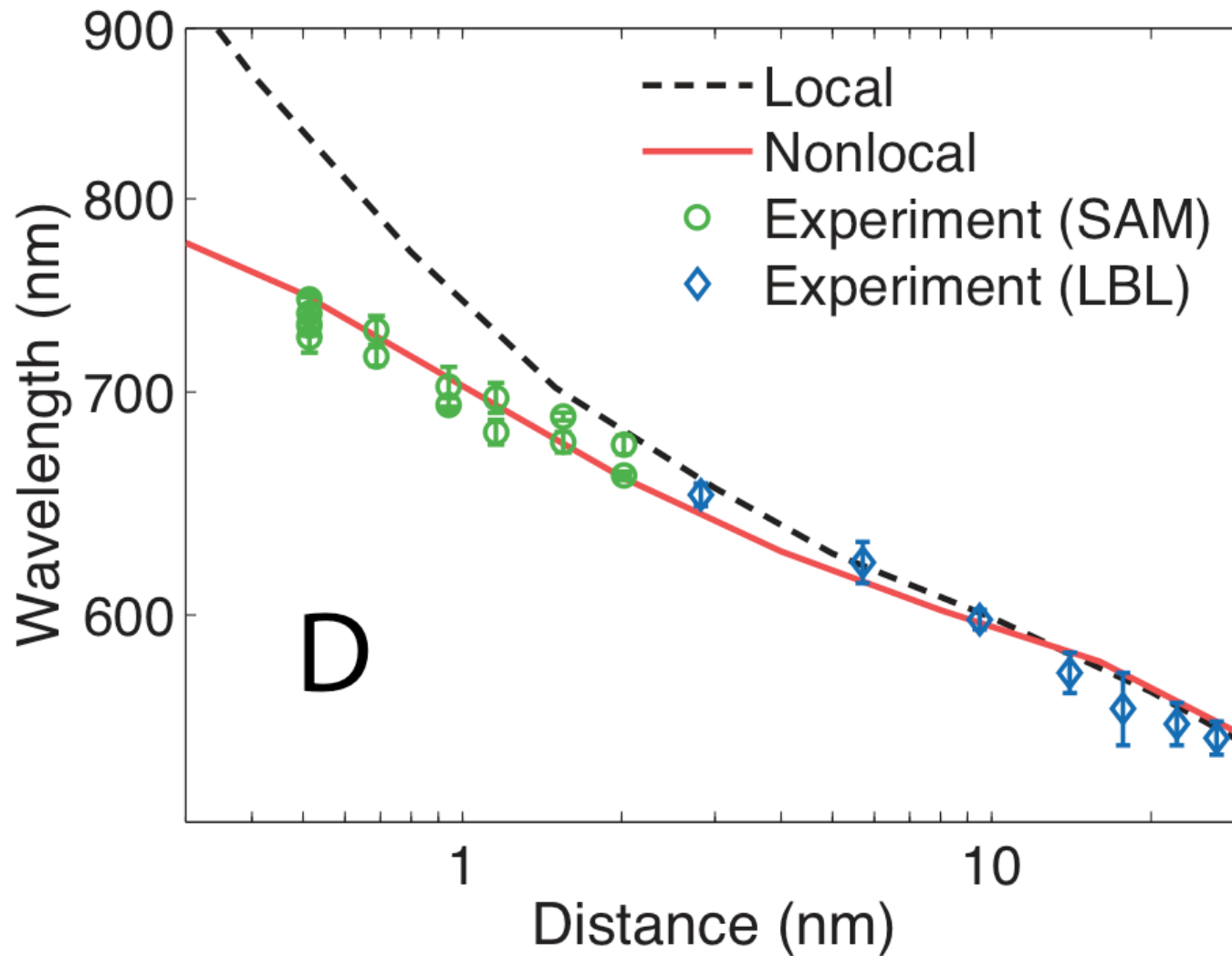
Simulation of a single film-coupled nanoparticle. **Left:** Relative electron surface density showing the excited surface plasmon polariton propagating over the metal film. **Right (top):** A plane wave is incident at 75° from normal. **Right (bottom):** The near-fields surrounding the nanosphere. Looking closer yet, it can be seen that the fields penetrate into the nanosphere a distance on the order of the Thomas-Fermi screening length.

Measuring non-locality – simulations II



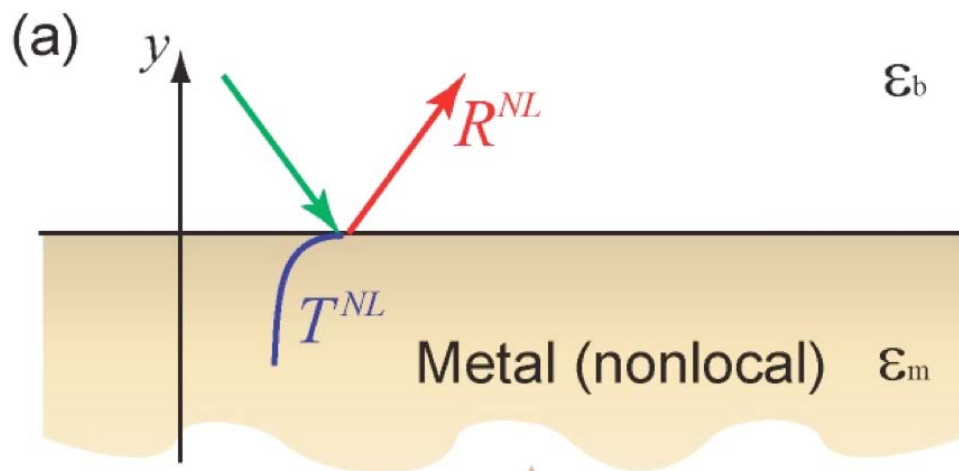
Resonant frequency (left), and local enhancement (right) at various sphere/surface separations of a gold nanosphere of radius r on a 300 nm thick film for various degrees of non locality.

Measuring non-locality: comparison with expt.



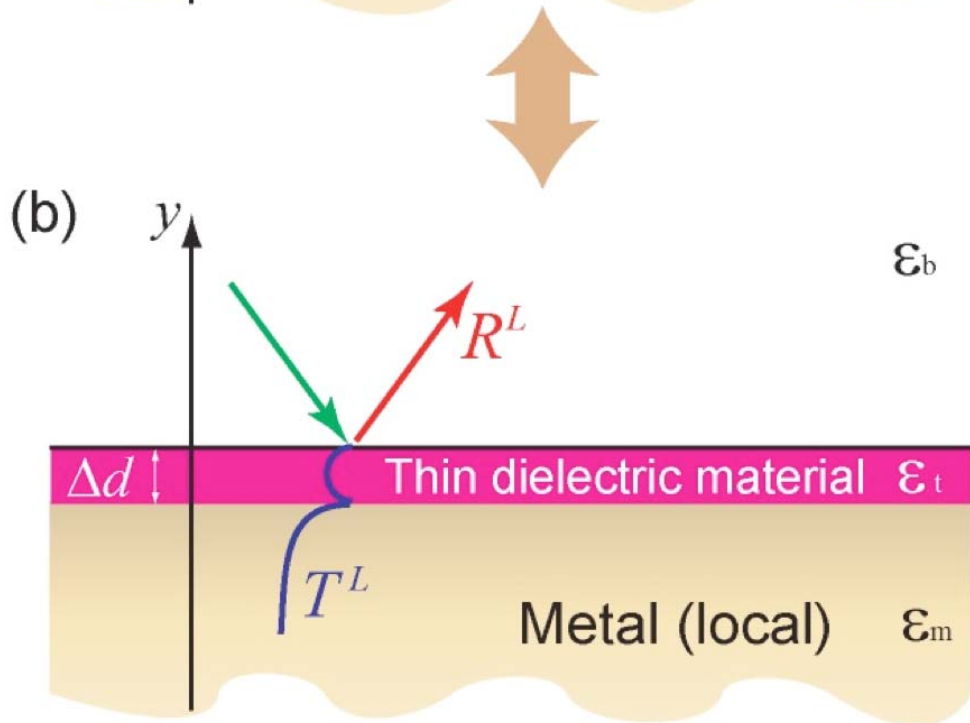
Comparison of experimental measurements from both SAM and LBL type spacers with numerical results with a best fit $\beta = 1.27 \times 10^6$ m/s. i.e. the polarisation charge penetrates $\delta \approx 0.6$ nm into the metal.

Non locality can be accurately modelled by a *local* dielectric layer

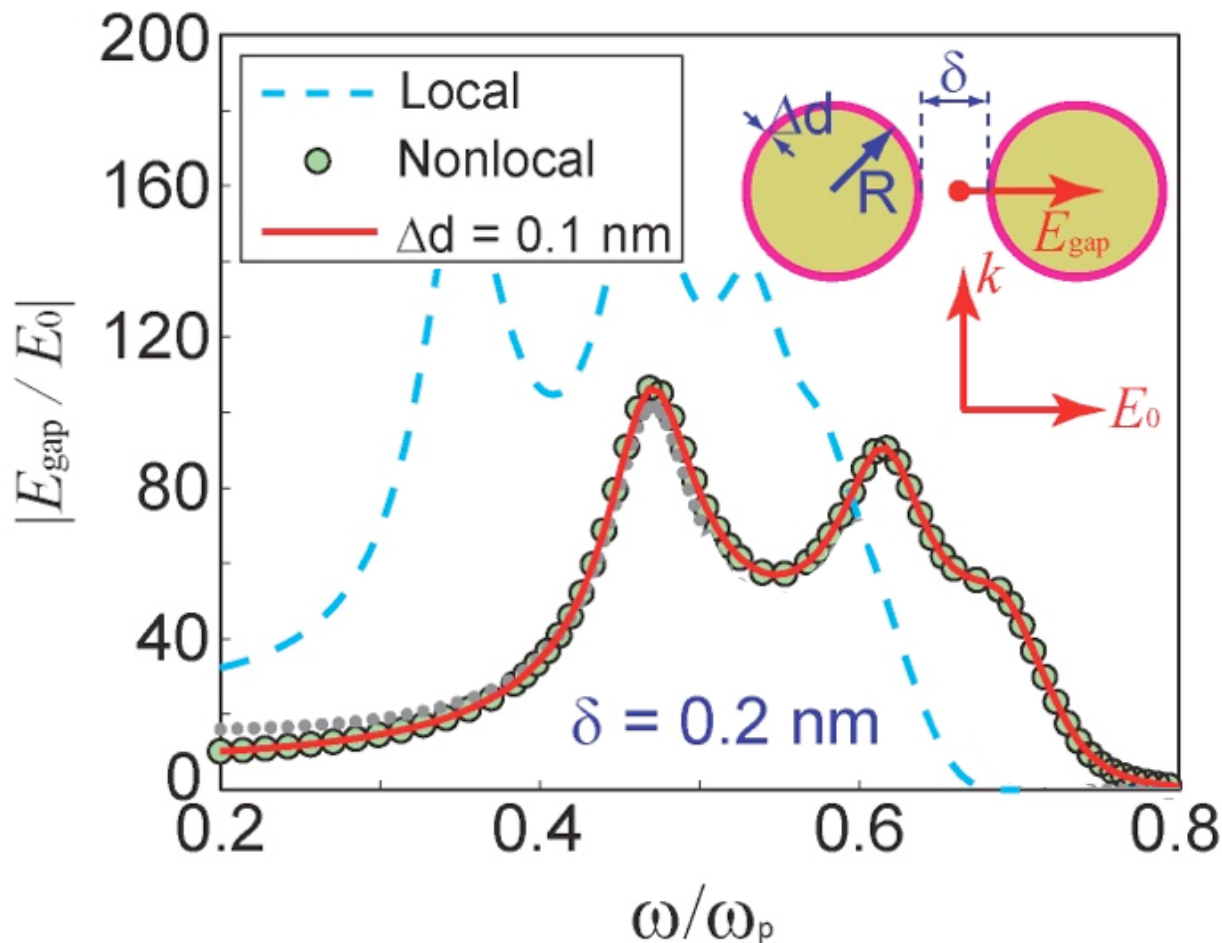


left top: in a nonlocal description surface charge is smeared out into the metal.

left bottom: the effect of the smearing has the same effect as a thin layer of dielectric coated onto the metal surface

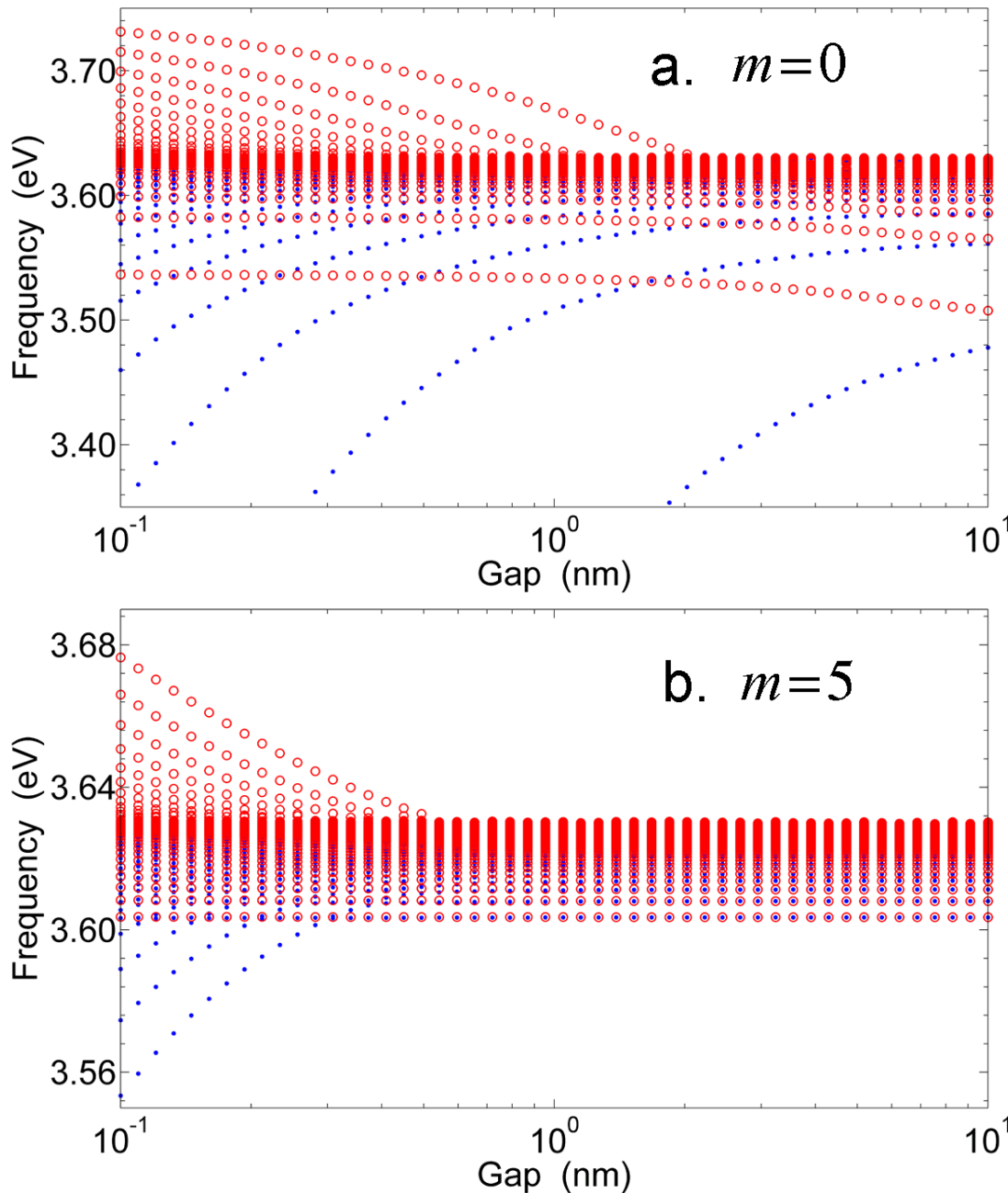


Non locality can be accurately modelled by a *local* dielectric layer



Electric field enhancement versus incident frequency for a pair of 10 nm radius gold nanowires separated by a $\delta = 0.2$ nm gap evaluated at the gap, comparing a full non-local calculation with the local dielectric layer model.

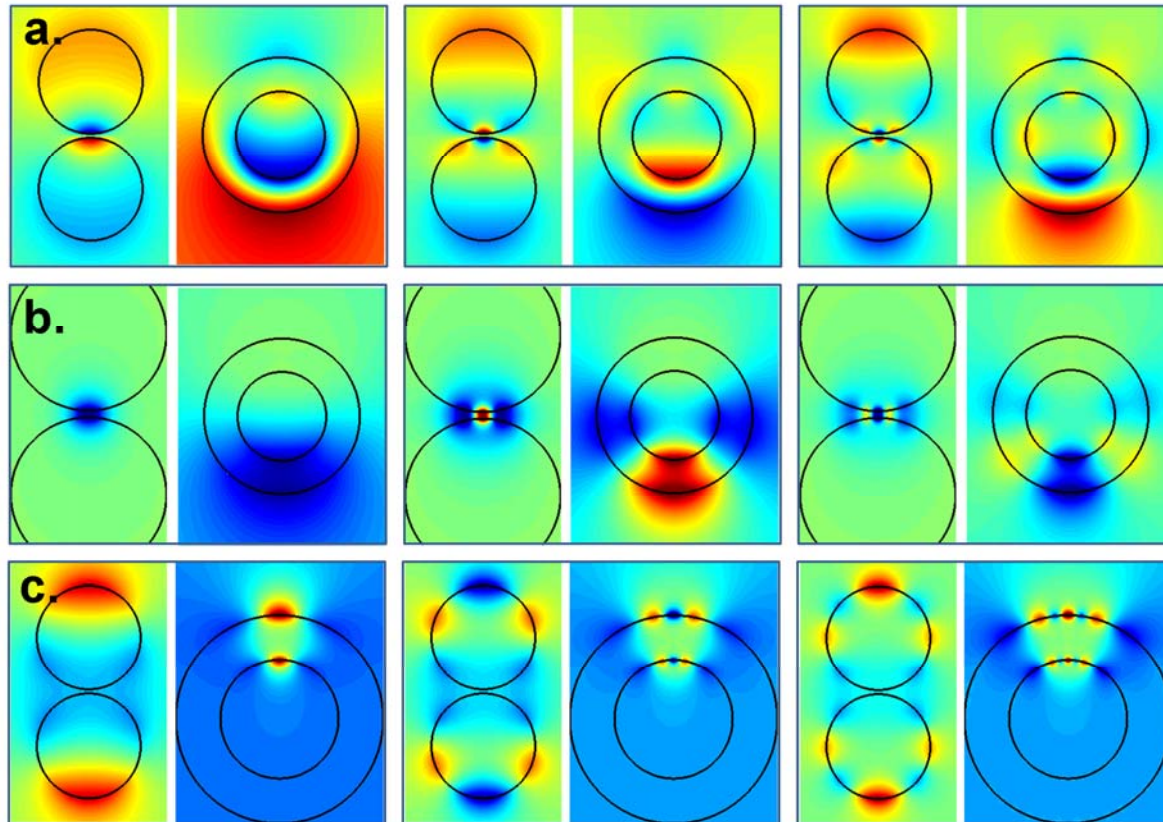
The modes of two nearly touching spheres



Modes of two 5 nm radius spheres for various separations a) for $m = 0$ and b) $m = 5$. The even modes are represented by open circles, the odd by closed circles. As the gap narrows the odd modes tend to zero frequency, $\varepsilon'_M(\omega = 0) = -\infty$, and some of the even modes tend to the bulk plasma frequency, $\varepsilon'_M(\omega = \omega_p) = 0$, where $\hbar\omega_p = 3.76$ eV for silver. The surface plasmon frequency is $\hbar\omega_{sp} = 3.63$ eV. However there is another set of even modes that tend to other intermediate limits.

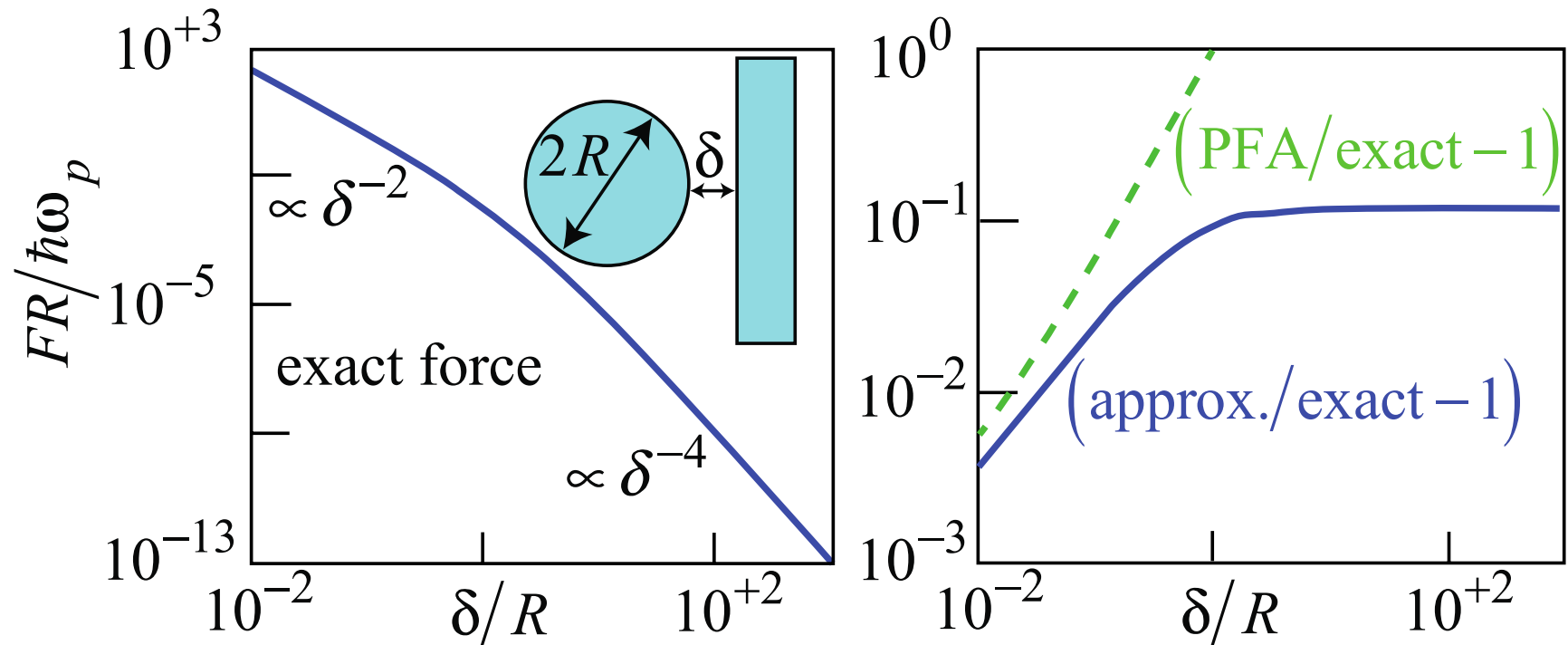


Extension to 3D – two spheres



The potential distribution shown in real space and in the transformed space for two spheres each 10nm in diameter, separated by 0.4nm. For all figures $m = 0$. Top: the odd modes at 3.536, 3.582, and 3.597eV; middle: the normal even modes at 3.703, 3.673, and 3.652eV; bottom: the anomalous even modes at 3.028, 3.418 and 3.523eV. Blue denotes the minimum potential, red the maximum, and green zero potential.

Exploiting T.O. to calculate Van der Waals forces



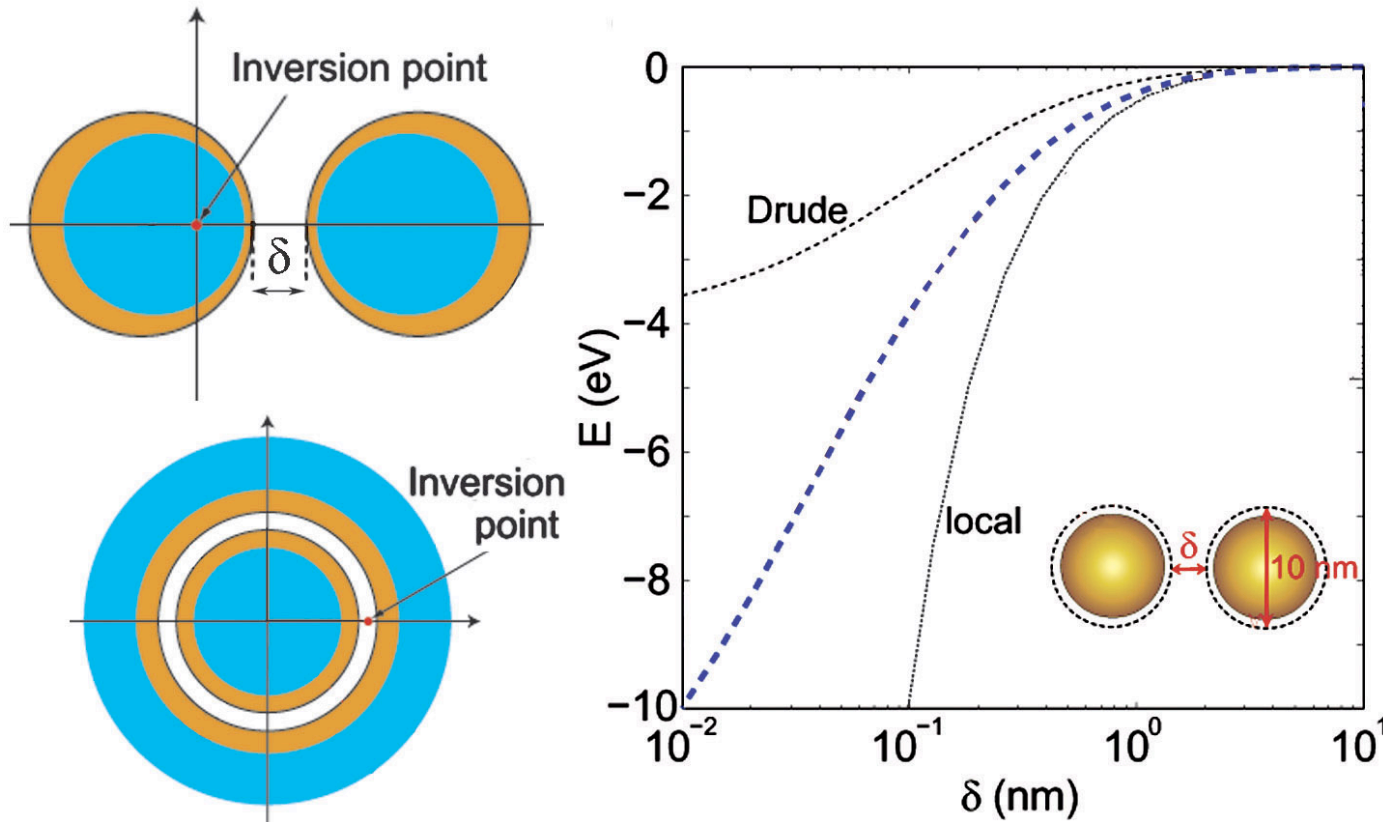
The Van der Waals force acting between a small metallic sphere and a metallic surface. The permittivity describes a plasmonic system.

Left: the fully converged exact force in units of $\hbar\omega_p/R$.

Right: deviation from the exact force of the proximity force approximation (PFA), and our analytic formula, which is accurate to 10% out to large distances, and extremely accurate at small distances.

van der Waals forces

work by Rongkuo Zhao & Yu Luo, PNAS 111 18422 (2014)



van der Waals energy between two 10-nm-diameter gold nanoparticles as a function of the separation. For the blue dashed line, nonlocal effects are considered. The black dotted line shows the van der Waals energy calculated neglecting nonlocal effects. The energy considering nonlocal effects but neglecting the Lorentzian terms in the permittivity is shown by the short dashed line.

Early work on electron energy loss spectra

J. Phys. C: Solid State Phys., Vol. 8, 1975. Printer in Great Britain. 1975

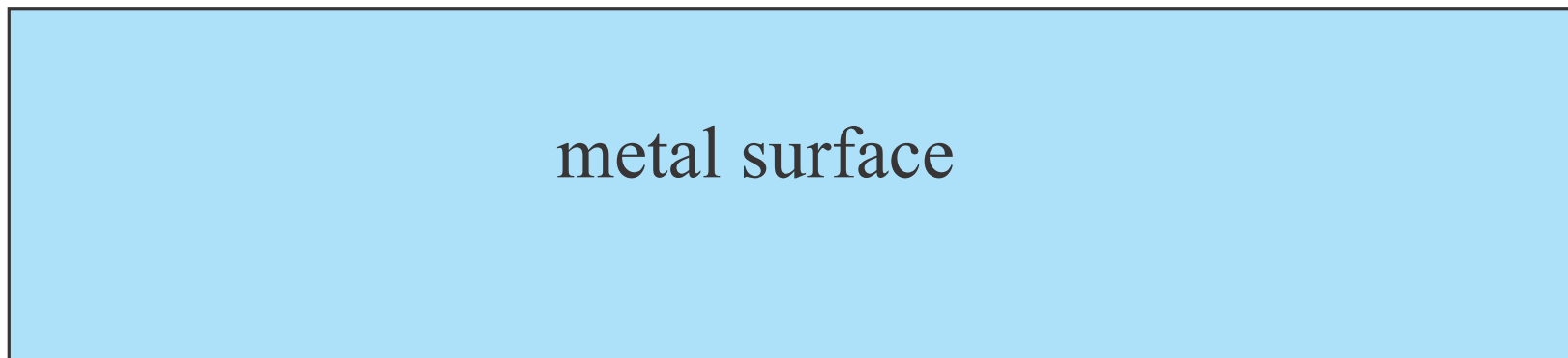
Absorption profile at surfaces

P M Echenique and J B Pendry

The Cavendish Laboratory, Madingley Road, Cambridge, UK

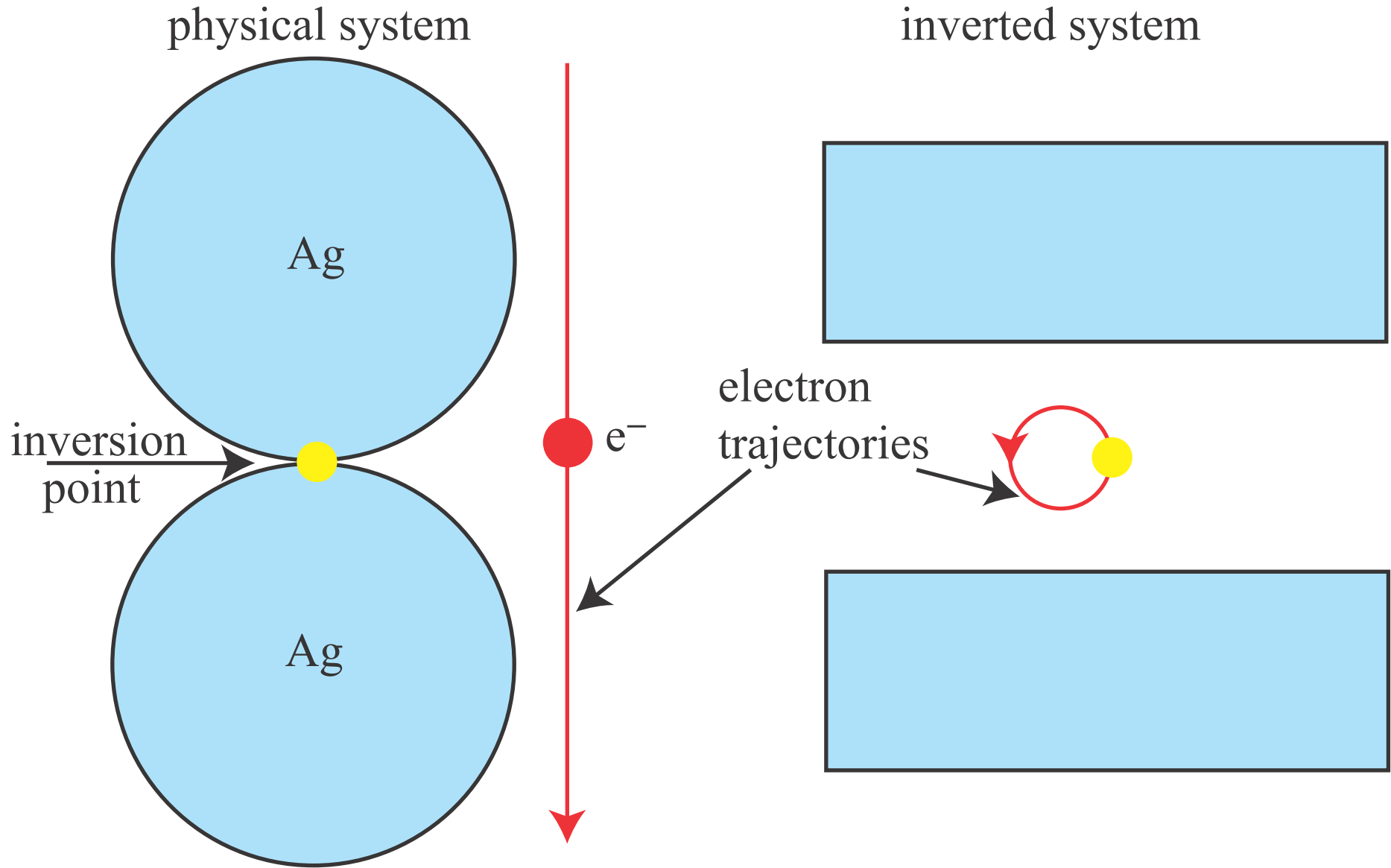
Received 21 April 1975

Abstract. Attenuation of the elastic component of an electron beam outside a surface is calculated. Significant attenuation is found in the case of RHEED experiments, explaining an earlier disagreement between theory and experiment observed by Menadue and Colella.



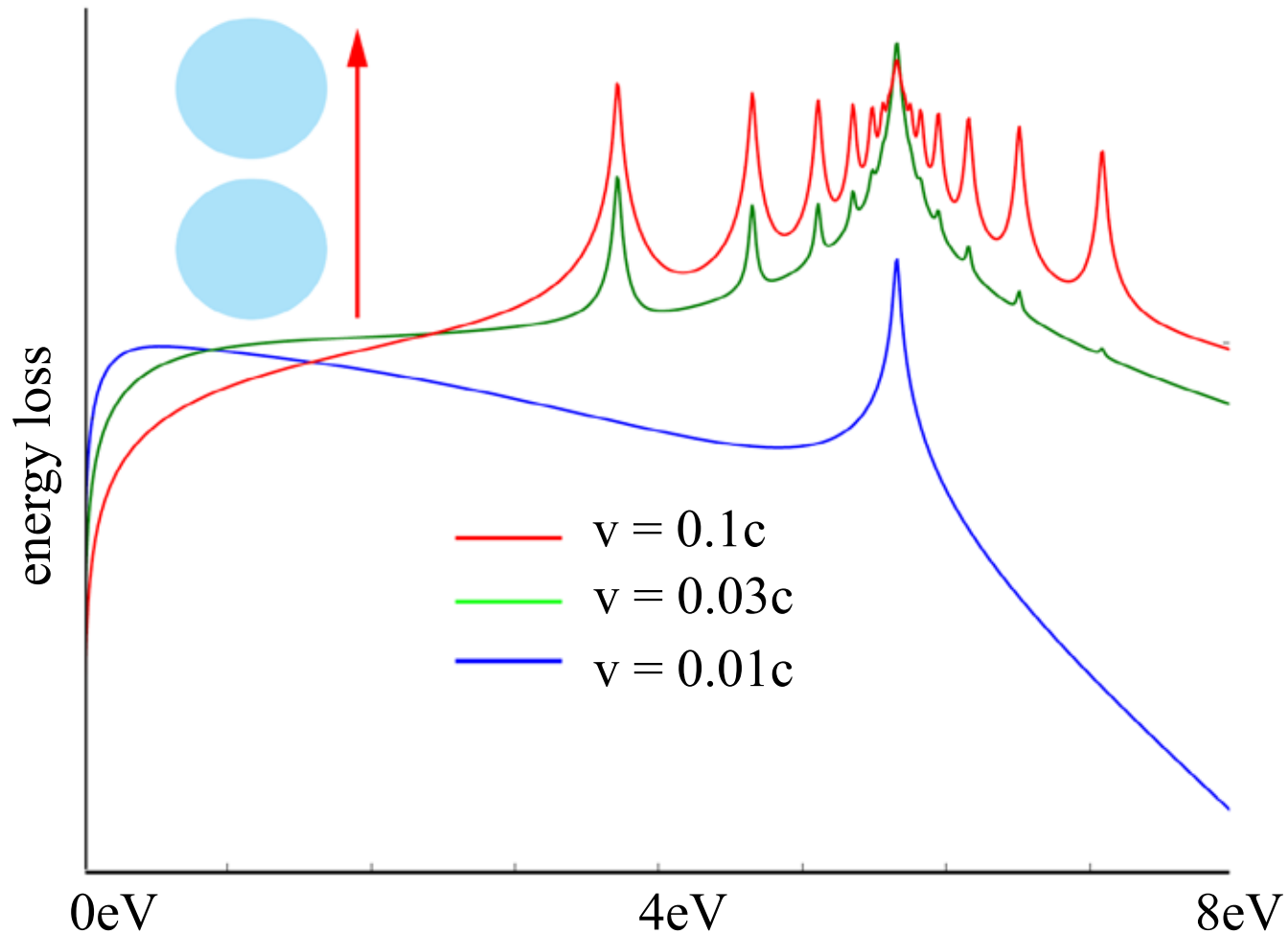
Applications of transformation optics - I

simplifying complex problems – two touching cylinders - $z' = 1/z$



Electron energy loss – work by Yu Luo

two silver nanowires radius 5nm, 0.1nm gap



Note: for electrons, unlike photons, there is no dipole selection rule, and all the modes are visible above and below the surface plasmon frequency

Applications of transformation optics - II

simplifying complex problems – a knife edge - $z' = \ln z$

